

# PARALLEL-IN-TIME PRECONDITIONERS FOR THE SINC-NYSTRÖM METHOD

JUN LIU\* AND SHU-LIN WU†

**Abstract.** The Sinc-Nyström method is a high-order numerical method based on Sinc basis functions for discretizing evolutionary differential equations in time. But in this method we have to solve all the time steps in one-shot (i.e. all-at-once), which results in a large-scale nonsymmetric dense system that is expensive to handle. In this paper, we propose and analyze preconditioner for such dense system arising from both the parabolic and hyperbolic PDEs. The proposed preconditioner is a low-rank perturbation of the original matrix and has two advantages. First, we show that the eigenvalues of the preconditioned system are highly clustered with some uniform bounds which are independent of the mesh parameters. Second, the preconditioner can be used parallel for all the Sinc time points via a block diagonalization procedure. Such a parallel potential owes to the fact that the eigenvector matrix of the diagonalization is well conditioned. In particular, we show that the condition number of the eigenvector matrix only mildly grows as the number of Sinc time points increases, and thus the roundoff error arising from the diagonalization procedure is controllable. The effectiveness of our proposed PinT preconditioners is verified by the observed mesh-independent convergence rates of the preconditioned GMRES in reported numerical examples.

**Key words.** Sinc-Nyström method, Parallel-in-time preconditioner, Kronecker product approximation, GMRES, diagonalization

**AMS subject classifications.** 65M55, 65M12, 65M15, 65Y05

**1. Introduction.** Belonging to the large family of pseudospectral methods, the Sinc-Nyström numerical method [43] is a special one among numerous high-order discretization schemes that can achieve an exponential order of accuracy for approximating ODEs/PDEs and integral equations [3, 4, 24, 38], even in the presence of boundary singularities and boundary layers<sup>1</sup>. Such a method lies in first transforming the initial-value ODE into a Volterra integral equation of the second kind and then applying the collocation approximation to the latter. Besides the exponential order of accuracy, the basis functions provide the computationally favorable Toeplitz structures of the discretization matrix  $\mathcal{A}$ , which will be used in this paper to facilitate the development of efficient preconditioner denoted by  $\mathcal{P}$ . However, for large-scale ODEs (such as the ones arise from semi-discretizing time-dependent PDEs in high dimension) the unknowns over all the collocation time points are fully coupled and this requires to solve a large-scale nonsymmetric dense system  $\mathcal{A}\mathbf{y}_h = \mathbf{b}_h$ , which is often very time consuming to solve. In this paper, we propose and analyze a structured preconditioner for handling this problem.

The novelty of the proposed preconditioner is twofold. First, as we will show in Section 3 the eigenvalues of the preconditioned matrix  $\mathcal{P}^{-1}\mathcal{A}$  are highly clustered for both the parabolic and hyperbolic problems, which indicates fast convergence of the preconditioned GMRES in practice (confirmed by numerical results in Section 4). Second, the preconditioner can be used in parallel for all the Sinc time points. We briefly explain such a parallel-in-time (PinT) implementation as follows. By diagonalizing  $\mathcal{P}$  as  $\mathcal{P} = \mathcal{V}\mathcal{D}\mathcal{V}^{-1}$  with a block diagonal matrix  $\mathcal{D}$  and  $\mathcal{V} = V \otimes I_n$ , we can compute  $\mathcal{P}^{-1}\mathbf{r}$  with any vector  $\mathbf{r}$  via three steps:

$$\mathbf{s}_1 := \mathcal{V}^{-1}\mathbf{r} = (V^{-1} \otimes I_n)\mathbf{r}, \quad \mathbf{s}_2 := \mathcal{D}^{-1}\mathbf{s}_1, \quad \mathcal{P}^{-1}\mathbf{r} = \mathcal{V}\mathbf{s}_2 = (V \otimes I_n)\mathbf{s}_2,$$

\*Department of Mathematics and Statistics, Southern Illinois University Edwardsville, Edwardsville, IL 62026, USA. E-mail: [juliu@siue.edu](mailto:juliu@siue.edu)

†School of Mathematics and Statistics, Northeast Normal University, Changchun 130024, China. E-mail: [wushulin84@hotmail.com](mailto:wushulin84@hotmail.com)

<sup>1</sup>The presence of boundary singularities and layers often dramatically deteriorates the expected approximation accuracy of the standard finite difference and finite element discretization schemes, although such a degradation can be mildly alleviated with adaptive meshing or local refined meshing techniques.

where  $V \in \mathbb{C}^{m \times m}$ ,  $I_n$  and  $I_m$  are identity matrices with  $m$  and  $n$  being respectively the number of collocation time points and the dimension of ODEs. (More details on these three steps will be supplied in Section 3.1.) The first and last steps only concern matrix-vector multiplications and thus the computation cost is relatively low (by taking into account the fact that  $m \ll n$  is not large in practice due to the exponential order of accuracy in time). The major computation is the second step for  $\mathbf{s}_2$ , but each diagonal block can be computed in parallel for all the  $m$  blocks. In the above three steps, we need to be cautious about the roundoff error arising from diagonalizing  $\mathcal{P}$ . Large roundoff error would seriously pollute the accuracy and according to the analysis in [13, 15] the roundoff error is proportional to the condition number of the eigenvector matrix  $V$ , i.e.,  $\text{Cond}_2(V)$ . For the proposed preconditioner  $\mathcal{P}$ , we show that  $\text{Cond}_2(V)$  is of moderate magnitude and only weakly grows as  $m$  increases.

Another contribution of this paper is a new strategy for applying the diagonalization-based preconditioner for nonlinear problems (or linear problems with time-varying coefficient matrix). For these problems, the widely used approach is the average-based Kronecker product approximation proposed in [12]. This approach works well if the variance of the Jacobian matrices over the time points is small. But if the variance is large, it may result in slow convergence or even divergence for the preconditioned GMRES method. Here, we use the *nearest Kronecker product approximation* (NKPA) technique for handling Jacobian matrices and numerical results indicate that the resulting NKPA-based preconditioner is much more effective than that obtained via the *averaging* approach in [12].

PinT algorithms for evolutionary problems attract considerable attentions in the last two decades [10], mainly due to the advent of massively parallel processors that provide a potential to significantly speed up the traditional sequential time-stepping schemes. Given the sequential nature of the forward time evolution, the development of effective PinT algorithms is more challenging than the counterparts in space. There are several different types of PinT algorithms in literature, such as the parareal algorithm [26], the multigrid reduction in time (MGRiT) algorithm [9], deferred correction methods [5, 37], and the diagonalization-based technique [29]. The mechanism of each algorithm varies greatly, which leads to significant difference in application scopes, convergence properties and parallel efficiency. In particular, the diagonalization-based technique which is built upon diagonalizing the time discretization matrix within the so-called all-at-once system shows promising speedup (see numerical results in [14, 16]). As we will see in Section 2, such an all-at-once system arises naturally in the Sinc-Nyström methods and therefore we continue to investigate such a technique in this paper. The diagonalization technique was first proposed by Maday and Rønquist in 2008 [29] and then followed by many authors [2, 6, 13, 16, 25, 27, 30, 41]. (A summary of the diagonalization-based PinT algorithms can be found in [14].) These previous work use the time-stepping method (e.g., the linear multistep methods or the Runge-Kutta method) and the time discretization matrix is a lower triangular Toeplitz matrix (the all-at-once matrix  $\mathcal{A}$  is of *block* version). In this case, it is natural to define the preconditioner  $\mathcal{P}$  as a block circulant matrix and many good properties of the time discretization matrix, such as the sparsity, Toeplitz structure and diagonal dominance, can be utilized for the spectral analysis of  $\mathcal{P}^{-1}\mathcal{A}$ . However, for the Sinc-Nyström method the time discretization matrix is a dense non-symmetric matrix and there is no clear structure for the all-at-once matrix  $\mathcal{A}$ , which leads to essential difficulty for constructing an efficient preconditioner and for analyzing the spectrum of  $\mathcal{P}^{-1}\mathcal{A}$ .

The rest of this paper is organized as follows. In Section 2, we introduce the Sinc-Nyström method for both linear and nonlinear initial-value ODEs, where the corresponding linear and nonlinear all-at-once systems are formulated. In Section 3, preconditioners for the heat equations and the wave equations are introduced, where the spectrum of the preconditioned systems are carefully estimated. In Section 4, we study the convergence performance of our proposed

preconditioners for both parabolic and hyperbolic PDEs and validate the spectrum analysis by several numerical experiments. We conclude this paper in Section 5.

**2. The Sinc-Nyström method and the all-at-once system.** Following the notations used in [36, 43], in this section we briefly revisit the Sinc-Nyström method for solving the linear and nonlinear initial-value ODEs. The involved structured matrices for the all-at-once system are given for facilitating the later development and analysis of the proposed preconditioner.

**2.1. The Sinc-Nyström method.** For a given positive constant  $d \in (0, \pi)$ , we define a strip domain  $\mathcal{D}_d$  in the complex plane and a single-exponential conforming map  $\phi(z)$

$$\mathcal{D}_d := \{z \in \mathbb{C} : |\operatorname{Im}(z)| < d\}, \quad \phi(z) := \ln \frac{z-a}{b-z}.$$

The function  $\phi(z)$  maps a finite interval  $(a, b)$  to  $(-\infty, \infty)$ . Define a domain  $\mathcal{D}$  from  $\mathcal{D}_d$  via

$$\mathcal{D} = \psi(\mathcal{D}_d) := \{z = \psi(\zeta) : \zeta \in \mathcal{D}_d\}, \quad \psi(z) := \phi^{-1}(z) = \frac{a + be^z}{1 + e^z}.$$

In this paper we will only consider the case that  $(a, b)$  is a bounded interval, i.e.,  $(a, b) = (0, T)$ , but unbounded time intervals can be addressed as well by using different conforming maps. We denote by  $\mathbf{H}(\mathcal{D})$  the family of analytic functions on  $\mathcal{D}$  and for a given  $h > 0$  we define the Wiener function space

$$\mathbf{W}(\pi/h) := \left\{ f \in \mathbf{H}(\mathbb{C}) : \int_{\mathbb{R}} |f(t)|^2 dt < \infty \text{ and } |f(z)| \leq Ce^{\pi|z|/h} \right\}, \quad (2.1)$$

where  $C > 0$  is a constant. The Sinc-Nyström method is based on the Sinc function on  $\mathbb{R}$

$$\operatorname{Sinc}(x) = \begin{cases} \frac{\sin(\pi x)}{\pi x}, & x \neq 0, \\ 1, & x = 0. \end{cases}$$

By shifting the Sinc function with a given  $h > 0$ , we can define the set of Sinc basis functions

$$S[j, h](x) := \operatorname{Sinc}(x/h - j), \quad j = 0, \pm 1, \pm 2, \dots,$$

which forms a complete orthogonal sequence in the Wiener function space  $\mathbf{W}(\pi/h)$ . Therefore, for any function  $u \in \mathbf{W}(\pi/h)$  we have the Sinc series expansion (also known as the Paley-Wiener theorem)

$$u(x) = \sum_{j=-\infty}^{\infty} u(jh)S[j, h](x),$$

which results in a practical numerical method after truncation by choosing  $M$  and  $h$  suitably

$$u(x) \approx \sum_{j=-M}^M u(jh)S[j, h](x).$$

In practice, we can approximate any function  $f(t)$  defined on a finite interval  $(a, b)$  through the function composition with the conformal map  $\phi$  as follows

$$f(t) \approx f_h(t) := \sum_{j=-M}^M f_j S[j, h] \circ \phi(t) := \sum_{j=-M}^M f(t_j) S[j, h](\phi(t)), \quad (2.2)$$

where  $f_j := f(t_j)$  are the interpolation points at the  $m = 2M + 1$  Sinc time points  $t_j = \psi(jh)$ ,  $j = -M, \dots, M$ . Since the basis functions  $S[j, h] \circ \phi(t)$  vanish at the end points  $t = a$  and  $t = b$ , the above Sinc approximation is not accurate near the end points if  $f(a) \neq 0$  and/or  $f(b) \neq 0$ . To handle  $f(a) \neq 0$  and/or  $f(b) \neq 0$ , the above approximation can be modified to

$$f(t) \approx \widehat{f}_h(t) := f_{-M} w_a(t) + f_N w_b(t) + \sum_{j=-M}^M (f_j - f_{-M} w_a(t_j) - f_N w_b(t_j)) S[j, h] \circ \phi(t), \quad (2.3)$$

where two auxiliary basis functions  $w_a(t) := (b-t)/(b-a)$  and  $w_b(t) := (t-a)/(b-a)$  are introduced to accommodate the possible nonzero end points. To use the above approximation for ODEs we also need the following integral form of (2.2):

$$\begin{aligned} \int_a^t f(s)ds &\approx \int_a^t f_h(s)ds = \sum_{j=-M}^M f_j \int_a^t S[j, h] \circ \phi(s)ds \\ &= \sum_{j=-M}^M f_j \psi'(jh) J[j, h] \circ \phi(t), \end{aligned} \quad (2.4)$$

where  $J[j, h](x) := h \left( \frac{1}{2} + \frac{1}{\pi} \int_0^{\pi(x/h-j)} \frac{\sin(\tau)}{\tau} d\tau \right)$ .

We next revisit exponential convergence results for the above two approximations. To this end, we introduce the following function space

$$\mathbf{H}^\infty(\mathcal{D}) := \{f \in \mathbf{H}(\mathcal{D}) : \sup_{z \in \mathcal{D}} |f(z)| < \infty\}.$$

For any positive constant  $\alpha \in (0, 1]$  and some constants  $C_1$  and  $C_2$ , let

$$\begin{aligned} \mathbf{L}_\alpha(\mathcal{D}) &:= \{f \in \mathbf{H}^\infty(\mathcal{D}) : |f(z)| \leq C_1 |(z-a)(b-z)|^\alpha\}, \\ \mathbf{M}_\alpha(\mathcal{D}) &:= \{f \in \mathbf{H}^\infty(\mathcal{D}) : |f(z) - f(a)| \leq C_2 |(z-a)|^\alpha \text{ and } |f(b) - f(z)| \leq C_2 |(b-z)|^\alpha\}. \end{aligned}$$

**THEOREM 2.1** ([43]). *Let  $f \in \mathbf{M}_\alpha(\psi(\mathcal{D}_d))$  with  $d \in (0, \pi)$  and  $M$  be a positive integer. By choosing  $h = \sqrt{\frac{\pi d}{\alpha M}}$ , there exists a constant  $C$  (independent of  $M$  and  $h$ ) such that*

$$\max_{a \leq t \leq b} |f(t) - \hat{f}_h(t)| \leq C \sqrt{M} \exp(-\sqrt{\pi d \alpha M}).$$

**THEOREM 2.2** ([35]). *Let  $f \in \mathbf{L}_\alpha(\psi(\mathcal{D}_d))$  with  $d \in (0, \pi)$  and  $M$  be a positive integer. By choosing  $h = \sqrt{\frac{\pi d}{\alpha M}}$ , there exists a constant  $C$  (independent of  $M$  and  $h$ ) such that*

$$\max_{a \leq t \leq b} \left| \int_a^t f(s)ds - \sum_{j=-M}^M f_j \psi'(jh) J[j, h] \circ \phi(t) \right| \leq C \exp(-\sqrt{\pi d \alpha M}).$$

**2.2. The all-at-once system.** We now introduce the Sinc-Nyström method to linear and nonlinear ODE systems and the resulting all-at-once system. Efficient computation of such a system plays a central role in the practical applications of this method.

**2.2.1. Linear time-varying ODEs.** We first consider the following initial value ODEs

$$y'(t) = K(t)y(t) + g(t), \quad y(0) = r \in \mathbb{R}^n, \quad t \in (0, T), \quad (2.5)$$

where  $y(t), g(t) \in \mathbb{R}^n$  are vector functions and  $K(t) \in \mathbb{R}^{n \times n}$  is a time-dependent coefficient matrix. Such ODEs can also be derived from semi-discretized parabolic and hyperbolic PDEs. To apply the Sinc-Nyström method, we first rewrite (2.5) into an integral equation

$$y(t) = r + \int_0^t \{K(s)y(s) + g(s)\} ds, \quad t \in (0, T).$$

According to (2.4), we get the Sinc-Nyström approximation of  $y(t)$  as

$$y^h(t) = r + \sum_{j=-M}^M \{K(t_j)y^h(t_j) + g(t_j)\} \psi'(jh) J[j, h] \circ \phi(t), \quad (2.6)$$

which, by collocating at the same  $m := 2M + 1$  time points  $\{t_l\}_{l=-M}^M$ , leads to

$$y^h(t_l) = r + \sum_{j=-M}^M \{K(t_j)y^h(t_j) + g(t_j)\} \psi'(jh) J[j, h] \circ \phi(t_l), \quad l = -M, \dots, M. \quad (2.7)$$

By definitions we have  $\psi'(jh) = 1/\phi'(t_j)$ ,  $\phi(t_l) = \phi(\psi(lh)) = lh$ , and

$$J[j, h](lh) = h \left( \frac{1}{2} + \int_0^{(l-j)} \frac{\sin(\pi t)}{\pi t} dt \right) =: h\sigma_{l-j}^{(-1)}.$$

Define the  $m \times m$  dense Toeplitz matrix

$$I^{(-1)} = [I_{l,j}^{(-1)}] := [\sigma_{l-j}^{(-1)}]_{l,j=1}^m = \left[ \frac{1}{2} + \int_0^{(l-j)} \frac{\sin(\pi t)}{\pi t} dt \right]_{l,j=1}^m,$$

whose (complex) eigenvalues lie in the open right half plane [20]. For any given scalar function  $g$ , define the  $m \times m$  diagonal matrix  $\mathbb{D}(g) = \text{diag}(g(t_{-M}), \dots, g(t_M))$  over the  $m$  time points. Let  $I_p \in \mathbb{R}^{p \times p}$  be an identity matrix of size  $p \times p$  and  $e_m = [1, 1, \dots, 1]^T \in \mathbb{R}^m$  be a column vector of all ones. We use  $(\cdot)^T$  and  $(\cdot)^*$  to denote the non-conjugate transpose and conjugate transpose, respectively. With the Kronecker product notations, the Sinc-Nyström discretization scheme (2.7) can be formulated into an all-at-once linear system after suitable ordering the unknowns

$$\mathcal{A}y_h := \left( I_m \otimes I_n - (I^{(-1)}D \otimes I_n)\mathbb{K} \right) y_h = b_h, \quad (2.8)$$

where  $y_h = [y(t_{-M}); \dots; y(t_M)] \in \mathbb{R}^{mn}$ ,  $g_h = [g(t_{-M}); \dots; g(t_M)] \in \mathbb{R}^{mn}$ ,  $f_h = e_m \otimes r \in \mathbb{R}^{mn}$ ,  $D = h\mathbb{D}(1/\phi')$  with  $1/\phi'(t) = t(T-t)/T > 0$ ,  $b_h = (I^{(-1)}D \otimes I_n)g_h + f_h$  and  $\mathbb{K}$  is a block-diagonal matrix given by

$$\mathbb{K} = \text{blockdiag}(K(t_{-M}), \dots, K(t_M)) \in \mathbb{R}^{mn \times mn}.$$

In the simple case of constant coefficient matrix  $K(t) = K$ , there obviously holds  $\mathbb{K} = I_m \otimes K$  and hence  $(I^{(-1)}D \otimes I_n)\mathbb{K} = (I^{(-1)}D \otimes I_n)(I_m \otimes K) = I^{(-1)}D \otimes K$ , which reduces (2.8) to

$$\mathcal{A}y_h := \left( I_m \otimes I_n - I^{(-1)}D \otimes K \right) y_h = b_h. \quad (2.9)$$

Under certain assumptions on  $K(t)$  and  $g(t)$ , it was shown in [21, 34, 43] that the linear all-at-once system (2.8) with a sufficiently large  $M$  is uniquely solvable and the obtained Sinc approximation  $\hat{y}^h(t)$  in the form of (2.3) converges to  $y(t)$  exponentially, i.e.,

$$\max_{0 \leq t \leq T} \|y(t) - \hat{y}^h(t)\|_\infty = O\left(\sqrt{M}e^{-\sqrt{\pi d \alpha M}}\right).$$

Although the exponential convergence of the above Sinc-Nyström discretization is well established, to the best of our knowledge the development of fast solvers for solving the all-at-once linear systems (2.8) and (2.9) were not addressed in literature so far. We note that an efficient solver for these all-at-once systems is crucial if the ODE system is very stiff and/or the ODE system is of large scale, such as the one derived from semi-discretizing time-dependent PDEs.

**2.2.2. Nonlinear ODEs.** We next consider the nonlinear ODEs

$$y'(t) = q(t, y(t)) + g(t), \quad y(0) = r \in \mathbb{R}^n, \quad t \in (0, T), \quad (2.10)$$

where  $q(t, y(t)) = [q_1(t, y(t)), q_2(t, y(t)), \dots, q_n(t, y(t))]^\top \in \mathbb{R}^n$ . The same Sinc-Nyström discretization of (2.10) leads to a system of nonlinear equations

$$y^h(t_l) = r + \sum_{j=-M}^M \{q(t_j, y^h(t_j)) + g(t_j)\} \psi'(jh) J[j, h] \circ \phi(t_l), \quad l = -M, \dots, M, \quad (2.11)$$

which can be formulated into the following all-at-once form

$$\mathcal{F}(\mathbf{y}_h) := (I_m \otimes I_n) \mathbf{y}_h - (I^{(-1)} D \otimes I_n) \mathbf{q}(\mathbf{y}_h) = (I^{(-1)} D \otimes I_n) \mathbf{g}_h + \mathbf{f}_h =: \mathbf{b}_h, \quad (2.12)$$

with the nonlinear part  $\mathbf{q}(\mathbf{y}_h) = [q(t_{-M}, y_{-M}); \dots; q(t_M, y_M)] \in \mathbb{R}^{mn}$  (here  $y_l = y^h(t_l)$ ). The Jacobian matrix of  $\mathcal{F}(\mathbf{y}_h)$  reads

$$\nabla \mathcal{F}(\mathbf{y}_h) = (I_m \otimes I_n) - (I^{(-1)} D \otimes I_n) \mathbf{Q}(\mathbf{y}_h), \quad (2.13)$$

where

$$\mathbf{Q}(\mathbf{y}_h) := \nabla_y \mathbf{q}(\mathbf{y}_h) = \text{blockdiag}(\nabla_y q(t_{-M}, y_{-M}), \dots, \nabla_y q(t_M, y_M)) \in \mathbb{R}^{mn \times mn} \quad (2.14)$$

is a block-diagonal matrix with  $\nabla_y q$  being the Jacobian matrix of  $q$  with respect to  $y$ , given by

$$\nabla_y q(t, y) := \begin{bmatrix} \frac{\partial q_1}{\partial y_1} & \frac{\partial q_1}{\partial y_2} & \dots & \frac{\partial q_1}{\partial y_n} \\ \frac{\partial q_2}{\partial y_1} & \frac{\partial q_2}{\partial y_2} & \dots & \frac{\partial q_2}{\partial y_n} \\ \vdots & \vdots & \ddots & \vdots \\ \frac{\partial q_n}{\partial y_1} & \frac{\partial q_n}{\partial y_2} & \dots & \frac{\partial q_n}{\partial y_n} \end{bmatrix} \in \mathbb{R}^{n \times n}.$$

Applying Newton's iteration to (2.12) leads to

$$\mathbf{y}_h^{(k+1)} = \mathbf{y}_h^{(k)} - [\nabla \mathcal{F}(\mathbf{y}_h^{(k)})]^{-1} (\mathcal{F}(\mathbf{y}_h^{(k)}) - \mathbf{b}_h), \quad k = 0, 1, 2, \dots \quad (2.15)$$

where  $\mathbf{y}_h^{(0)}$  is the initial guess. We see that the Jacobian matrix  $\nabla \mathcal{F}(\mathbf{y}_h^{(k)})$  in (2.15) has the same structure as (2.8) and therefore a preconditioner for (2.8) is also applicable to (2.15) as well. For convergence of the above Newton iteration, a variant of the well-known Newton-Kantorovich theorem is given in [43, p. 344, Theorem 6.4.4]. In general, the Newton iteration achieves only local convergence within a short time window and to handle a much longer time interval we can first split the whole time interval into several subintervals and then apply the Newton iterations to these subintervals one after another.

**3. The preconditioner and the spectrum analysis.** In this section, we first propose a PinT preconditioner  $\mathcal{P}$  for solving the all-at-once system (2.8) and then we give a spectral analysis for the preconditioned matrix  $\mathcal{P}^{-1} \mathcal{A}$ . We start by discussing the simple constant coefficient case (2.9), where the all-at-once matrix is

$$\mathcal{A} = I_m \otimes I_n - I^{(-1)} D \otimes K. \quad (3.1)$$

The preconditioner for  $\mathcal{A}$  is different for the case  $\sigma(K) \subset \mathbb{R}$  and  $\sigma(K) \subset i\mathbb{R}$ , where  $\sigma(K)$  denotes the spectrum of  $K$ . We note that these are two representative cases: the first case represents that the differential equation is dissipative while the second case corresponds to wave propagation problems (e.g.,  $K$  is the discrete matrix of a wave equation).

**3.1. The preconditioner for the case  $\sigma(K) \subset \mathbb{R}$ .** In view of the special Toeplitz structure of  $I^{(-1)}$  in  $\mathcal{A}$ , we propose the following preconditioner

$$\mathcal{P} = I_m \otimes I_n - SD \otimes K, \quad (3.2)$$

where the Toeplitz matrix  $I^{(-1)}$  is approximated by its skew-symmetric part [33]:

$$S = \frac{I^{(-1)} - (I^{(-1)})^\top}{2}.$$

A routine calculation shows that  $S$  is skew-circulant and skew-symmetric (i.e.  $S^\top = -S$ ). Moreover, it holds

$$S_{k,l} = \frac{1}{2} \int_{l-k}^{k-l} \frac{\sin(\pi t)}{\pi t} dt = \int_0^{k-l} \frac{\sin(\pi t)}{\pi t} dt = \sigma_{k-l}^{(-1)} - \frac{1}{2},$$

and hence  $S$  is a rank-one perturbation of  $I^{(-1)} = \left[ \sigma_{k-j}^{(-1)} \right]_{k,j=1}^m$  according to

$$S = I^{(-1)} - \frac{1}{2} e_m e_m^\top \text{ with } e_m := [1, 1, \dots, 1]^\top. \quad (3.3)$$

So  $\mathcal{P}$  is a rank- $n$  perturbation of  $\mathcal{A}$  and it is anticipated to be an effective preconditioner of  $\mathcal{A}$ . In [1], it was shown that  $S$  is unitary diagonalizable and all the eigenvalues of  $S$  are simple. Furthermore, in [20, Theorem 2.1] it was shown that  $(S + \epsilon e_m e_m^\top)$  (including  $I^{(-1)}$  as a special case) is nonsingular for any  $\epsilon > 0$  and has all its eigenvalues lie in the open right half-plane.

**3.1.1. Implementation details.** Since the skew-symmetric matrix  $S$  is diagonalizable and  $SD$  is similar to the skew-symmetric matrix  $D^{\frac{1}{2}}SD^{\frac{1}{2}}$ , the matrix  $SD$  is also diagonalizable. Let  $SD = V\Sigma V^{-1}$  be its diagonalization (or eigen-decomposition). Then we can factorize  $\mathcal{P}$  as

$$\mathcal{P} = (V \otimes I_n) (I_m \otimes I_n - \Sigma \otimes K) (V^{-1} \otimes I_n).$$

Hence, for any vector  $\mathbf{r}$  the preconditioning step  $\mathbf{s} = \mathcal{P}^{-1}\mathbf{r}$  can be computed by three steps:

$$\begin{aligned} \text{Step-(i)} \quad \mathbf{s}_1 &= \text{mat}(\mathbf{r})(V^{-1})^\top \in \mathbb{R}^{n \times m}, \\ \text{Step-(ii)} \quad \mathbf{s}_2(:,j) &= (I_n - \lambda_j K)^{-1} \mathbf{s}_1(:,j), \quad j = 1, 2, \dots, m, \\ \text{Step-(iii)} \quad \mathbf{s} &= \text{vec}(\mathbf{s}_2 V^\top) \in \mathbb{R}^{mn}, \end{aligned} \quad (3.4)$$

where  $\Sigma = \text{diag}(\lambda_1, \dots, \lambda_m)$  and  $\mathbf{s}_{1,2}(:,j)$  denotes the  $j$ -th column of  $\mathbf{s}_{1,2}$ . In (3.4), we have used the reshaping operations: matrix-to-vector  $\text{vec}$  and vector-to-matrix  $\text{mat}$ . Clearly, the  $m$  independent linear systems in Step-(ii) can be computed in parallel.

**REMARK 3.1.** For the preconditioner  $\mathcal{P}$  in (3.2) there is a more convenient implementation of  $\mathcal{P}^{-1}\mathbf{r}$ . We can factorize  $\mathcal{P}$  as  $\mathcal{P} = (D^{-\frac{1}{2}} \otimes I_n) \left( I_m \otimes I_n - D^{\frac{1}{2}}SD^{\frac{1}{2}} \otimes K \right) (D^{\frac{1}{2}} \otimes I_n)$  with  $D^{\frac{1}{2}}SD^{\frac{1}{2}}$  being skew-symmetric since

$$\left( D^{\frac{1}{2}}SD^{\frac{1}{2}} \right)^\top = D^{\frac{1}{2}}S^\top D^{\frac{1}{2}} = - \left( D^{\frac{1}{2}}SD^{\frac{1}{2}} \right).$$

This implies that  $D^{\frac{1}{2}}SD^{\frac{1}{2}}$  is a normal matrix and it is unitary diagonalizable:  $D^{\frac{1}{2}}SD^{\frac{1}{2}} = W\Sigma W^*$  with a unitary matrix  $W$ . Therefore, we can replace  $V^{-1}$  in (3.4) by  $W^*D^{\frac{1}{2}}$ , i.e., there is no need to invert the eigenvector matrix.

One may wonder why we do not directly factorize  $I^{(-1)}D$  and then solve the all-at-once system  $\mathcal{A}\mathbf{y}_h = \mathbf{b}_h$  by the above diagonalization procedure? This is indeed the most convenient approach but unfortunately it does not work due to large roundoff errors arising from

diagonalization of  $I^{(-1)}D$ . According to the analysis in [13, 15], the roundoff errors for the diagonalization procedure (3.4) is proportional to the condition number of the eigenvector matrix  $V$  (denoted by  $\text{Cond}_2(V)$ ). A very large  $\text{Cond}_2(V)$  leads to large roundoff error that will seriously pollute the accuracy of obtained numerical solution. Let  $U$  and  $V$  be respectively the eigenvector matrix of  $I^{(-1)}D$  and  $SD$ . In Figure 3.1, we compare the condition number for  $U$  and  $V$  as a function of system size  $M$ . Here, we use the `eig` function in MATLAB for both  $U$  and  $V$ . Clearly,  $\text{Cond}_2(V)$  is much smaller than  $\text{Cond}_2(U)$  and the former seems increases only linearly. The condition number  $\text{Cond}_2(U)$  grows exponentially as  $M$  increases. Our numerical simulations indicate that if we directly solve the all-at-once system  $\mathcal{A}$  by utilizing the diagonalization  $I^{(-1)}D = U\Psi U^{-1}$ , the unavoidable large roundoff error seriously pollutes the solution accuracy for  $M \geq 64$  (see the last column of Table 4.4 in Section 4).

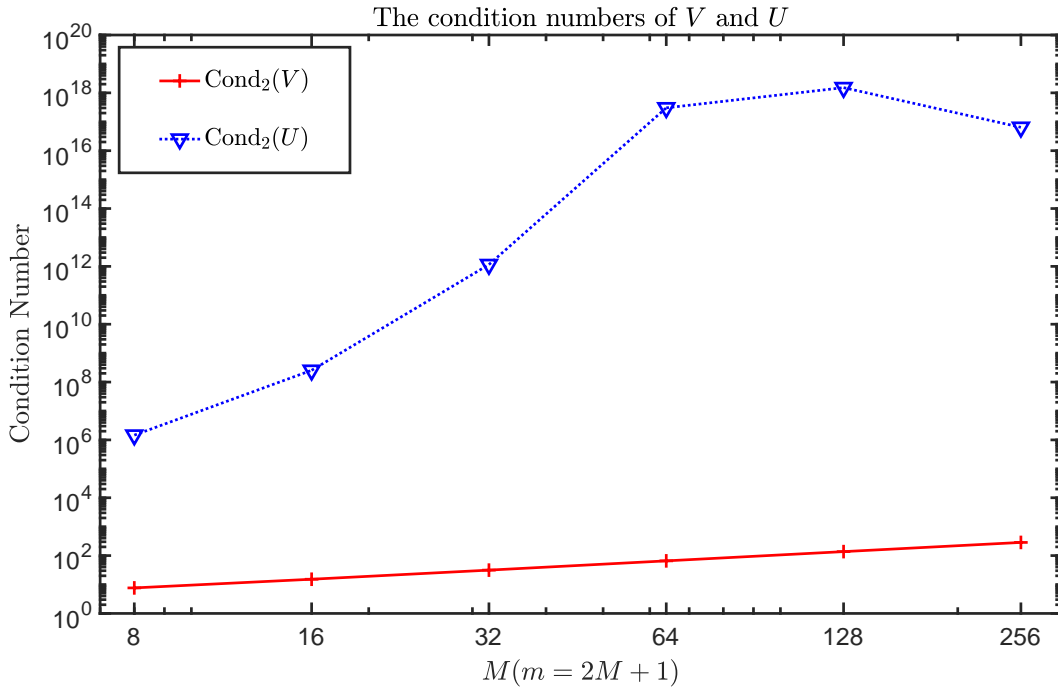


FIG. 3.1. The growth of  $\text{Cond}_2(U)$  and  $\text{Cond}_2(V)$  with  $U$  and  $V$  being the eigenvector matrix of  $I^{(-1)}D$  and  $SD$ , respectively. The huge condition number (over  $10^{15}$  for  $M \geq 64$ ) of  $U$  implies that we can not directly invert  $\mathcal{A}^{-1}\mathbf{b}_h$  by the diagonalization technique, because the roundoff errors will seriously pollute the solution accuracy. The mildly increasing condition number of  $V$  will not contaminate the approximation accuracy.

The following lemma presents an estimate of  $\text{Cond}_2(V)$ , but it seems rather pessimistic compared to the numerical result shown in Figure 3.1. We mention that the eigenvector matrix  $V$  is not unique because  $V\Phi$  is also an eigenvector matrix with any nonsingular diagonal matrix  $\Phi$ . Hence it is entirely impossible to improve the following estimate with some suitable scaling matrix  $\Phi$ . We however do not further pursue this goal in the current paper.

LEMMA 3.1. Let  $V\Sigma V^{-1}$  be a diagonalization of  $SD$ . It holds  $\text{Cond}_2(V) = O(e^{\sqrt{M}})$ .

*Proof.* It follows from  $SD = V\Sigma V^{-1}$  and  $D^{\frac{1}{2}}SD^{\frac{1}{2}} = W\Sigma W^*$  that  $V = D^{-\frac{1}{2}}W$ . Since  $W$  is unitary with  $W^{-1} = W^*$ , there holds

$$\text{Cond}_2(V) = \|V\|_2 \|V^{-1}\|_2 = \|D^{-\frac{1}{2}}W\|_2 \|W^* D^{\frac{1}{2}}\|_2 = \|D^{-\frac{1}{2}}\|_2 \|D^{\frac{1}{2}}\|_2 = \text{Cond}_2(D^{\frac{1}{2}}).$$



Recall that  $t_{-M} = \psi(-Mh) = \frac{Te^{-Mh}}{1+e^{-Mh}}$  and  $h = \sqrt{\frac{\pi d}{\alpha M}}$  (chosen in Theorem 2.1), it holds that

$$\text{Cond}_2(D^{\frac{1}{2}}) = \sqrt{\text{Cond}_2(D)} = \sqrt{\frac{T^2/4}{t_{-M}(T-t_{-M})}} = e^{Mh/2}(1+e^{-Mh})/2 = O\left(e^{\sqrt{M}}\right).$$

Hence,  $\text{Cond}_2(V) = \text{Cond}_2(D^{\frac{1}{2}}) = O\left(e^{\sqrt{M}}\right)$ .  $\square$

**3.1.2. Spectrum analysis of  $\mathcal{P}^{-1}\mathcal{A}$ .** We now analyze the eigenvalues of  $\mathcal{P}^{-1}\mathcal{A}$  for the case with constant coefficient. In general, a clustered spectrum of  $\mathcal{P}^{-1}\mathcal{A}$  indicates the effectiveness of the preconditioner  $\mathcal{P}$  in practice, although the rigorous convergence rate of the preconditioned GMRES is not conclusively determined by the spectrum alone (see e.g. [19, 32, 46]), especially for non-normal systems.

For simplicity, we assume that  $K$  can be diagonalized as  $K = Q\Gamma Q^{-1}$ , which is often the case if  $K$  is the discrete matrix of self-adjoint elliptic operator, e.g., the Laplacian. With  $K = Q\Gamma Q^{-1}$  we get the following factorization of  $\mathcal{A}$  and  $\mathcal{P}$

$$\begin{aligned}\mathcal{A} &= (I_m \otimes Q)(I_m \otimes I_n - I^{(-1)}D \otimes \Gamma)(I_m \otimes Q^{-1}), \\ \mathcal{P} &= (I_m \otimes Q)(I_m \otimes I_n - SD \otimes \Gamma)(I_m \otimes Q^{-1}).\end{aligned}$$

The following lemma will be used to estimate the spectrum of  $\mathcal{P}^{-1}\mathcal{A}$ .

LEMMA 3.2. *Let  $z(\mu) := e_m^\top (\mu^{-1}D^{-1} + I^{(-1)})^{-1} e_m$ . It holds  $z(\mu) \in [0, 2)$  for  $\mu \geq 0$ .*

*Proof.* For  $\mu = 0$ , the result holds trivially since  $z(0) = 0$ . Hence, we will only discuss the case  $\mu > 0$ . For this case we first prove that  $z(\mu)$  is well-defined, i.e.,  $\mu^{-1}D^{-1} + I^{(-1)}$  is nonsingular. To this end, we let  $(\lambda, \xi)$  with  $\|\xi\|_2 = 1$  be any (complex) eigenpair of  $\mu^{-1}D^{-1} + I^{(-1)}$ , that is  $\lambda\xi = (\mu^{-1}D^{-1} + I^{(-1)})\xi = (\mu^{-1}D^{-1} + S + \frac{1}{2}e_me_m^\top)\xi$ . Since  $\|\xi\|_2 = 1$ , it holds

$$\lambda = \lambda\|\xi\|_2^2 = \lambda\xi^*\xi = \mu^{-1}\xi^*D^{-1}\xi + \xi^*S\xi + \frac{1}{2}\xi^*e_me_m^\top\xi = \mu^{-1}\xi^*D^{-1}\xi + \xi^*S\xi + \frac{1}{2}\|e_m^\top\xi\|_2^2.$$

By noticing that  $\xi^*D^{-1}\xi > 0$  (due to the fact that  $D = h\mathbb{D}(1/\phi')$  is diagonal with positive entries) and  $\xi^*S\xi$  is purely imaginary (due to  $S^* = S^\top = -S$ ), we have

$$\Re(\lambda) = \mu^{-1}\xi^*D^{-1}\xi + \frac{1}{2}\|e_m^\top\xi\|_2^2 > 0.$$

Hence,  $\mu^{-1}D^{-1} + I^{(-1)}$  is indeed nonsingular, i.e.,  $z(\mu)$  is well-defined.

Let  $\Phi_\mu := \mu^{-1}D^{-1} + S$ . Then following the proof for  $\mu^{-1}D^{-1} + I^{(-1)}$  we can show that  $\Phi_\mu$  is nonsingular for  $\mu > 0$  as well. By using the Sherman-Worrison-Woodbury formula [17],

$$\left(\mu^{-1}D^{-1} + I^{(-1)}\right)^{-1} = \left(\Phi_\mu + \frac{1}{2}e_me_m^\top\right)^{-1} = \Phi_\mu^{-1} - \frac{\Phi_\mu^{-1}e_me_m^\top\Phi_\mu^{-1}}{2 + e_m^\top\Phi_\mu^{-1}e_m}, \quad (3.5)$$

which implies

$$z(\mu) = e_m^\top\Phi_\mu^{-1}e_m - \frac{(e_m^\top\Phi_\mu^{-1}e_m)^2}{2 + e_m^\top\Phi_\mu^{-1}e_m} = \frac{2e_m^\top\Phi_\mu^{-1}e_m}{2 + e_m^\top\Phi_\mu^{-1}e_m} = 2 - \frac{4}{2 + e_m^\top\Phi_\mu^{-1}e_m}. \quad (3.6)$$

Let  $\gamma(\mu) := e_m^\top\Phi_\mu^{-1}e_m$  and  $v := \Phi_\mu^{-1}e_m$ . Then it holds  $v \neq 0$  and  $e_m = \Phi_\mu v$ , which, using the fact that  $S$  is skew-symmetric with  $v^\top Sv = 0$ , leads to

$$v^\top e_m = v^\top (\mu^{-1}D^{-1} + S)v = \mu^{-1}v^\top D^{-1}v.$$

This together with the fact that  $D = h\mathbb{D}(1/\phi')$  is diagonal with positive entries and

$$\gamma(\mu) = e_m^\top \Phi_\mu^{-1} e_m = e_m^\top v = (e_m^\top v)^\top = v^\top e_m$$

gives  $\gamma(\mu) = \mu^{-1} v^\top D^{-1} v > 0$  for  $\mu > 0$ . In view of (3.6), we obtained the desired result  $z(\mu) = 2 - \frac{4}{2+\gamma(\mu)} \in [0, 2)$ .  $\square$

As a numerical illustration of Lemma 3.2, in Figure 3.2 we plot the function  $z(\mu)$  with different  $M$  for  $\mu > 0$ . We see that  $z(\mu) \rightarrow 2$  as  $\mu \rightarrow \infty$  for a fixed  $M$ , but how fast  $z(\mu)$  approaches 2 seems to highly depend on  $M$ .

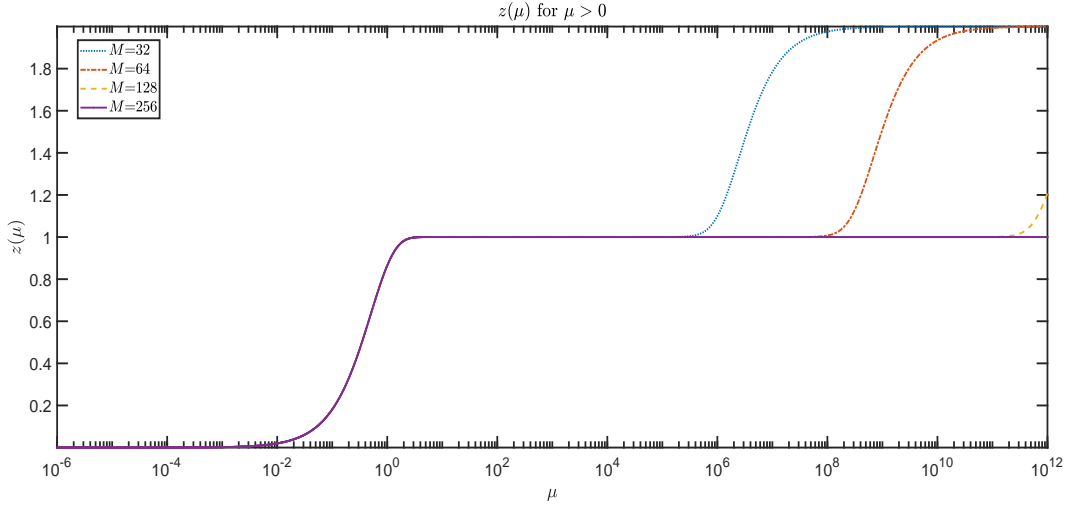


FIG. 3.2. The function  $z(\mu)$  for  $\mu \in [10^{-6}, 10^{12}]$  with different  $M$ . Here we take  $T = 2$ ,  $d = \pi/2$  and  $\alpha = 1$ .

**THEOREM 3.3.** *Suppose  $K$  is diagonalizable with negative spectrum  $\sigma(K) \subset (-\infty, 0)$ . Then,  $\mathcal{P}^{-1}\mathcal{A}$  has  $n(m-1)$  unity eigenvalues and  $n$  non-unity eigenvalues. Moreover, it holds*

$$\sigma(\mathcal{P}^{-1}\mathcal{A}) \subset [1, \infty).$$

*Proof.* Let  $-\mu \in \sigma(K)$  with  $\mu > 0$  be an arbitrary eigenvalue of  $K$ . Then, it is clear that

$$\sigma(\mathcal{P}^{-1}\mathcal{A}) = \sigma\left((I_m \otimes I_n - SD \otimes \Gamma)^{-1}(I_m \otimes I_n - I^{(-1)}D \otimes \Gamma)\right) = \bigcup_{-\mu \in \sigma(K)} \sigma(P_\mu^{-1}A_\mu),$$

where  $P_\mu = I_m + \mu SD = \mu \Phi_\mu D$ ,  $A_\mu = I_m + \mu I^{(-1)}D = \mu(\Phi_\mu + \frac{1}{2}e_m e_m^\top)D$  and  $\Phi_\mu = \mu^{-1}D^{-1} + S$ . (In the proof of Lemma 3.2 we have already proved that  $\Phi_\mu$  is nonsingular and thus  $P_\mu$  is nonsingular as well.) Since  $S = I^{(-1)} - \frac{1}{2}e_m e_m^\top$ , by the Sherman-Worrison-Woodbury formula [17] we have

$$P_\mu^{-1}A_\mu = \left(A_\mu - \frac{\mu}{2}e_m e_m^\top D\right)^{-1} A_\mu = I_m - A_\mu^{-1}e_m \left(-\frac{2}{\mu} + e_m^\top D A_\mu^{-1} e_m\right)^{-1} e_m^\top D,$$

which is a rank-one perturbation of the identity matrix. Hence  $P_\mu^{-1}A_\mu$  has  $(m-1)$  unity eigenvalues and the remaining only one non-unity eigenvalue is given by

$$\lambda_{\max}(P_\mu^{-1}A_\mu) = 1 - \frac{e_m^\top D A_\mu^{-1} e_m}{-\frac{2}{\mu} + e_m^\top D A_\mu^{-1} e_m} = \frac{2}{2 - \mu e_m^\top D A_\mu^{-1} e_m} = \frac{2}{2 - z(\mu)}, \quad (3.7)$$

where we have used the fact

$$\mu e_m^T D A_\mu^{-1} e_m = \mu e_m^T D (I_m + \mu I^{(-1)} D)^{-1} e_m = e_m^T \left( \mu^{-1} D^{-1} + I^{(-1)} \right)^{-1} e_m = z(\mu). \quad (3.8)$$

From Lemma 3.2, we have  $z(\mu) \in [0, 2)$  for  $\mu > 0$  and hence  $\lambda_{\max}(P_\mu^{-1} A_\mu) = \frac{2}{2-z(\mu)} \geq 1$ , which completes the proof.  $\square$

In Figure 3.3, we plot the computed eigenvalues of  $\mathcal{A}$  and  $\mathcal{P}^{-1}\mathcal{A}$  for the 1D heat equation (cf. Example 1 in Section 4). From Figure 3.3 we see that the eigenvalues of  $\mathcal{P}^{-1}\mathcal{A}$  are real (if neglecting the roundoff errors) and highly clustered around 1 (within a bounded interval  $[1.75, 2]$ ). Our numerical results in Table 4.1 show that the preconditioned GMRES converges in only a few iterations.

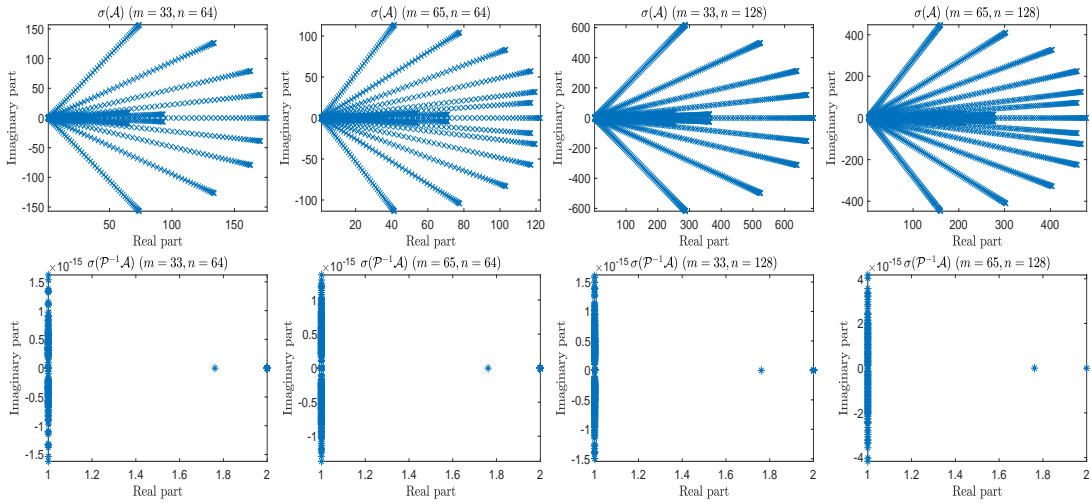


FIG. 3.3. The eigenvalues of  $\mathcal{A}$  and  $\mathcal{P}^{-1}\mathcal{A}$  for Example 2 in Section 4, i.e., 1D heat equation with  $n = 64, 128$  and  $m = 33, 65$ . Note that  $m(n-1)$  eigenvalues of  $\mathcal{P}^{-1}\mathcal{A}$  are one and all eigenvalues are real.

REMARK 3.2. From (3.7) the maximum of  $z(\mu) \in [0, 2)$  controls the upper bound of the eigenvalues of  $P_\mu^{-1} A_\mu$ . From Figure 3.2, we know that  $z(\mu) \rightarrow 2$  as  $\mu$  gets larger and hence  $\lambda_{\max}(P_\mu^{-1} A_\mu)$  may become large as well. Numerically, due to the highly clustering of the eigenvalues of  $\mathcal{P}^{-1}\mathcal{A}$  with real negative spectrum  $\sigma(K)$ , a few very large eigenvalues do not seem to cause obvious degeneration of convergence rate for the preconditioned GMRES method.

**3.2. The preconditioner for  $\sigma(K) \subset i\mathbb{R}$ .** We now consider the wave propagation problems, i.e.,  $\sigma(K) \subset i\mathbb{R}$ . In this case, the matrix  $\Phi_\mu$  defined in Lemma 3.2 (i.e.,  $\Phi_\mu := \mu^{-1} D^{-1} + S$ ) could be singular for some special  $\mu$  (the singularity of  $\Phi_\mu$  implies singularity of  $P_\mu = \mu \Phi_\mu D$  or equivalently  $\mathcal{P}$ ). In fact, for any purely imaginary eigenvalue  $i\tilde{\mu}$  of  $S^{\frac{1}{2}} D S^{\frac{1}{2}}$  we can choose  $\mu = \pm i\tilde{\mu}^{-1}$  such that the matrix  $\Phi_\mu$  is singular. Hence, generally speaking the preconditioner  $\mathcal{P}$  proposed in Section 3.1 is not applicable to wave propagation problems.

The above discussion motivates us to propose and study an improved preconditioner which actually works very well for both the parabolic and wave equations. The new preconditioner is a generalized version of  $\mathcal{P}$  parameterized by a small parameter  $\omega \in (0, 1)$  which is used to control the norm (or magnitude) of the rank-one perturbation term in constructing  $\mathcal{P}$ :

$$\mathcal{P}(\omega) = I_m \otimes I_n - (S(\omega)D) \otimes K, \quad (3.9)$$

where  $S(\omega)$  is defined as a damped rank-one perturbation of  $I^{(-1)}$ :

$$S(\omega) = I^{(-1)} - \frac{\omega}{2} e_m e_m^\top = S + \frac{1-\omega}{2} e_m e_m^\top, \quad \omega \in (0, 1). \quad (3.10)$$

When  $\omega$  is small (e.g.  $\omega = 0.01$ ) the preconditioner  $\mathcal{P}(\omega)$  is expected to perform better than  $\mathcal{P} = \mathcal{P}(1)$  in view of  $\lim_{\omega \rightarrow 0} \mathcal{P}(\omega) = \mathcal{A}$ . Suppose  $S(\omega)D$  is diagonalizable with  $S(\omega)D = V_\omega \Sigma_\omega V_\omega^{-1}$ , we expect that the condition number  $\text{Cond}_2(V_\omega)$  ranges from  $\text{Cond}_2(V)$  to  $\text{Cond}_2(U)$ , where  $U$  is the eigenvector matrix of  $I^{(-1)}D$ . With the diagonalization of  $S(\omega)D$ , the computation of  $\mathcal{P}^{-1}(\omega)\mathbf{r}$  is the same as the 3-step procedure (3.4) and we omit the presentation.

The growth of  $\text{Cond}_2(V_\omega)$  as  $M$  increases is illustrated in Figure 3.4, where  $\text{Cond}_2(V_\omega)$  seems to be proportional to  $\frac{1}{\omega} \text{Cond}_2(V)$ . (Unlike the preconditioner  $\mathcal{P}$  proposed in Section 3.1, the analysis of  $\text{Cond}_2(V_\omega)$ —even though a rough estimate as given by Lemma 3.1 for  $\mathcal{P}$ , is extremely difficult.) This implies that the roundoff error arising from the diagonalization procedure would be well controlled by choosing a moderate  $\omega$ . The remained question is how the parameter  $\omega$  influences the spectrum of the preconditioned matrix  $\mathcal{P}^{-1}(\omega)\mathcal{A}$ .

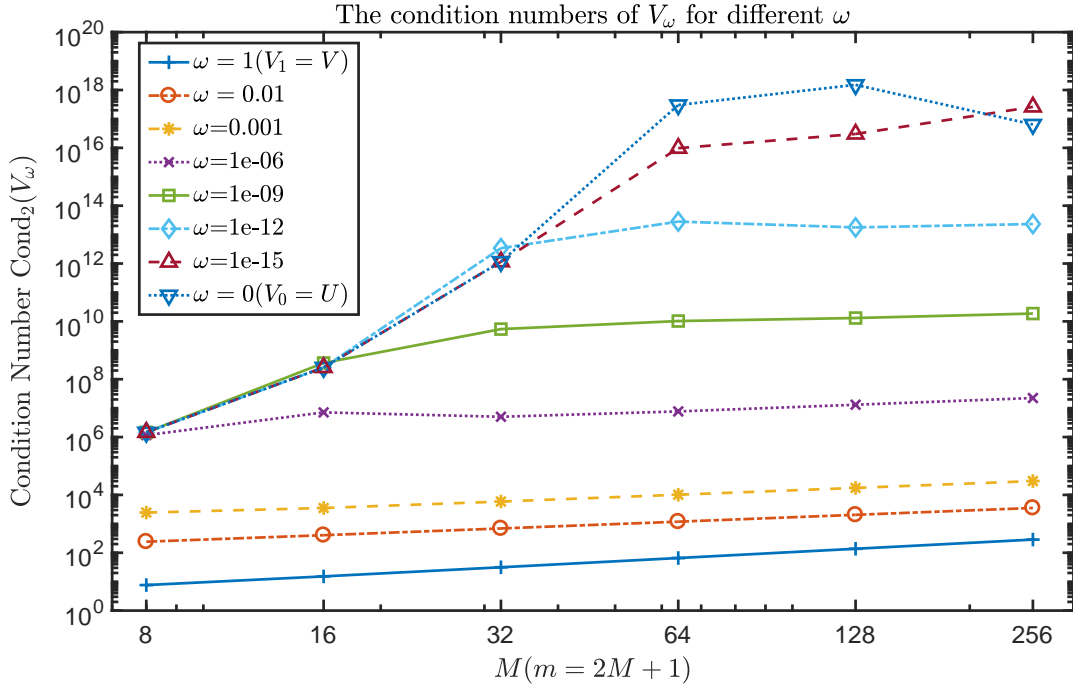


FIG. 3.4. The growth of the condition number  $\text{Cond}_2(V_\omega)$  as a function of  $M$  for different  $\omega$  values.

**THEOREM 3.4** (the case  $\sigma(K) \subset \mathbb{R}^-$ ). *Let  $K$  be a diagonalizable matrix with real negative eigenvalues. Then  $\mathcal{P}^{-1}(\omega)\mathcal{A}$  with  $\omega \in (0, 1)$  has only  $n$  non-unity eigenvalues and*

$$\sigma(\mathcal{P}^{-1}(\omega)\mathcal{A}) \in \left[1, \frac{1}{1-\omega}\right).$$

*Proof.* Following the proof arguments of Theorem 3.3, it is clear that

$$\sigma(\mathcal{P}^{-1}(\omega)\mathcal{A}) = \bigcup_{-\mu \in \sigma(K)} \sigma(P_\mu^{-1}(\omega)A_\mu),$$

where  $P_\mu(\omega) = I_m + \mu S(\omega)D = \mu(\mu^{-1}D^{-1} + S(\omega))D$  is nonsingular for  $\mu > 0$  since  $S(\omega)$  is nonsingular with all eigenvalues located in the open right half-plane. Since  $S(\omega) = I^{(-1)} - \frac{\omega}{2}e_m e_m^\top$ , by the Sherman-Worrison-Woodbury formula [17] we have

$$P_\mu^{-1}(\omega)A_\mu = \left(A_\mu - \frac{\mu\omega}{2}e_m e_m^\top D\right)^{-1} A_\mu = I_m - A_\mu^{-1}e_m \left(-\frac{2}{\mu\omega} + e_m^\top D A_\mu^{-1} e_m\right)^{-1} e_m^\top D,$$

which implies that  $P_\mu^{-1}(\omega)A_\mu$  has  $(m-1)$  unity eigenvalues and only one non-unity eigenvalue

$$\lambda(P_\mu^{-1}(\omega)A_\mu) = 1 - \frac{e_m^\top D A_\mu^{-1} e_m}{-\frac{2}{\mu\omega} + e_m^\top D A_\mu^{-1} e_m} = \frac{2}{2 - \omega\mu e_m^\top D A_\mu^{-1} e_m} =: \frac{2}{2 - \omega z(\mu)}, \quad (3.11)$$

where  $z(\mu)$  is the same function defined by Lemma 3.2 satisfying  $z(\mu) \in [0, 2)$  for  $\mu > 0$ . Hence

$$\lambda(P_\mu^{-1}(\omega)A_\mu) = \frac{2}{2 - \omega z(\mu)} \in \left[1, \frac{1}{1 - \omega}\right),$$

where together with other unity eigenvalues completes the proof.  $\square$

For the case that the eigenvalues of  $K$  are purely imaginary, we have the following uniform bounds for the spectrum of  $\mathcal{P}^{-1}(\omega)\mathcal{A}$ .

**THEOREM 3.5** (the case  $\sigma(K) \subset i\mathbb{R}$ ). *Let  $K$  be a diagonalizable matrix with purely imaginary spectrum  $\sigma(K)$ . Then  $\mathcal{P}^{-1}(\omega)\mathcal{A}$  with  $\omega \in (0, 1)$  has only  $n$  non-unity eigenvalues and*

$$\sigma(\mathcal{P}^{-1}(\omega)\mathcal{A}) \subset \mathbb{A}_\omega := \left\{z \in \mathbb{C} : \frac{\omega}{(2-\omega)} \leq \left|z - \frac{2}{2-\omega}\right| \leq \frac{\omega}{(2-\omega)(1-\omega)}\right\}.$$

*Proof.* We first claim that  $P_\mu(\omega) = I_m + \mu S(\omega)D$  is nonsingular for  $\mu \in i\mathbb{R}$ , which implies that the preconditioner  $\mathcal{P}(\omega)$  is invertible. If  $\mu = 0$ , the claim holds trivially. Hence we only have to consider  $\mu \neq 0$ . Since  $\mu \in i\mathbb{R}$ , it is sufficient to prove that any eigenvalue of  $S(\omega)D$  has non-zero real part. This is further equivalent to proving that any eigenvalue of  $D^{\frac{1}{2}}S(\omega)D^{\frac{1}{2}}$  has non-zero real part, since  $S(\omega)D$  is similar to  $D^{\frac{1}{2}}S(\omega)D^{\frac{1}{2}}$ . Since  $S$  is a skew-symmetric matrix (and thus  $S$  is diagonalizable) and  $S(\omega) = S + \frac{1-\omega}{2}e_m^\top e_m$  is a rank-one perturbation of  $S$ , from [31, Theorem 2.3] we know that  $S(\omega)$  is diagonalizable for any  $\omega \in (0, 1)$ . This implies that the eigenvectors of  $S(\omega)$ , denoted by  $\{v_1, v_2, \dots, v_m\}$ , forms a basis of  $\mathbb{C}^m$ . Without loss of generality, we assume that these eigenvectors are orthonormal basis of  $\mathbb{C}^m$  (after the Gram-Schmidt orthogonalization and normalization). Moreover, we assume that the eigenvalue associated with  $v_j$  is  $\lambda_j$ . From [20, Theorem 2.1] we know that these eigenvalues lie in the open right half-plane, that is  $\Re(\lambda_j) > 0$  for  $j = 1, 2, \dots, m$ . Hence, for any vector  $z \in \mathbb{C}^m$  expressed as  $z = c_1 v_1 + c_2 v_2 + \dots + c_m v_m$  it holds that

$$\Re(z^* S(\omega)z) = \Re(\lambda_1 |c_1|^2 + \lambda_2 |c_2|^2 + \dots + \lambda_m |c_m|^2) > 0. \quad (3.12)$$

Let  $(\lambda, \xi)$  is an eigenpair of  $D^{\frac{1}{2}}S(\omega)D^{\frac{1}{2}}$ , i.e.,  $D^{\frac{1}{2}}S(\omega)D^{\frac{1}{2}}\xi = \lambda\xi$ , with  $\xi \neq 0$ . we have

$$\xi^* D^{\frac{1}{2}}S(\omega)D^{\frac{1}{2}}\xi = \lambda \|\xi\|_2^2.$$

Now, by letting  $z = D^{\frac{1}{2}}\xi$  in (3.12) it follows that  $\Re(\xi^* D^{\frac{1}{2}}S(\omega)D^{\frac{1}{2}}\xi) > 0$  and therefore  $\lambda$  has non-zero real part.

Let  $z(\mu) = e_m^\top (\mu^{-1}D^{-1} + I^{(-1)})^{-1} e_m$ . Using the same notations in Theorem 3.4, we have

$$\sigma(\mathcal{P}^{-1}(\omega)\mathcal{A}) = \bigcup_{-\mu \in \sigma(K)} \sigma(P_\mu^{-1}(\omega)A_\mu) = \underbrace{\{1, 1, \dots, 1\}}_{n(m-1)} \cup \left\{ \frac{2}{2 - \omega z(\mu)} : -\mu \in \sigma(K) \right\},$$

We next prove the following relationship for  $\mu \in i\mathbb{R}$

$$|z(\mu) - 1| = 1. \quad (3.13)$$

Let  $w := (\mu^{-1}D^{-1} + I^{(-1)})^{-1}e_m$ , which gives  $(\mu^{-1}D^{-1} + S + \frac{1}{2}e_me_m^\top)w = e_m$ . Multiplying from left by the conjugate transpose  $w^*$ , we get

$$\mu^{-1}w^*D^{-1}w + w^*Sw + \frac{1}{2}w^*e_me_m^\top w = w^*e_m.$$

Notice that  $z(\mu) = e_m^\top w = (w^*e_m)^*$ , we get

$$\underbrace{\mu^{-1}w^*D^{-1}w + w^*Sw}_{=: \rho i} + \frac{1}{2}z^*(\mu)z(\mu) = z^*(\mu),$$

where  $(\mu^{-1}w^*D^{-1}w + w^*Sw) = \rho i$  with  $\rho \in \mathbb{R}$  holds because  $\mu \in i\mathbb{R}$  and  $S$  is skew-symmetric. Let  $z(\mu) = \Re(z(\mu)) + i\Im(z(\mu))$ . Then the above equation gives

$$\rho i + \frac{1}{2}\Re(z(\mu))^2 + \frac{1}{2}\Im(z(\mu))^2 = \Re(z(\mu)) - i\Im(z(\mu)),$$

which leads to (by matching the real part)  $\Re(z(\mu))^2 + \Im(z(\mu))^2 = 2\Re(z(\mu))$ , that is

$$(\Re(z(\mu)) - 1)^2 + \Im(z(\mu))^2 = 1,$$

i.e., the relationship (3.13) holds.

By (3.13), for any  $\mu \in i\mathbb{R}$  we have  $z(\mu) - 1 = e^{i\theta}$  with some  $\theta \in [0, 2\pi]$ . Hence

$$\frac{\omega}{(2-\omega)} \leq \left| \frac{2}{2-\omega z(\mu)} - \frac{2}{2-\omega} \right| = \frac{|2\omega e^{i\theta}|}{(2-\omega)|((2-\omega) - \omega e^{i\theta})|} \leq \frac{\omega}{(2-\omega)(1-\omega)},$$

where we have used  $|e^{i\theta}| = 1$  and the triangle inequality

$$2 - 2\omega = (2-\omega) - \omega|e^{i\theta}| \leq |((2-\omega) - \omega e^{i\theta})| \leq (2-\omega) + \omega|e^{i\theta}| = 2.$$

Hence, all the  $n$  non-unity eigenvalues of  $\mathcal{P}^{-1}(\omega)\mathcal{A}$  can be bounded by an annulus centered at  $(\frac{2}{2-\omega}, 0)$  with outer radius  $\frac{\omega}{(2-\omega)(1-\omega)}$  and inner radius  $\frac{\omega}{(2-\omega)}$ , that is

$$\sigma(\mathcal{P}^{-1}(\omega)\mathcal{A}) \subset \mathbb{A}_\omega := \left\{ z \in \mathbb{C} : \frac{\omega}{(2-\omega)} \leq \left| z - \frac{2}{2-\omega} \right| \leq \frac{\omega}{(2-\omega)(1-\omega)} \right\},$$

which together with  $1 \in \mathbb{A}_\omega$  completes the proof.  $\square$

In Figures 3.5 and 3.6 we plot the eigenvalues of  $\mathcal{P}^{-1}(\omega)\mathcal{A}$  for the linear heat equation and wave equation with  $\omega = 0.1$ , respectively. For the heat equation, all the eigenvalues are real and located within an interval  $[1, 1.11]$  as estimated in Theorem 3.4. For the wave equation, we see from Figure 3.6 that the eigenvalues are located within an annulus with a very narrow bandwidth. In both cases, the spectrum  $\sigma(\mathcal{P}^{-1}(\omega)\mathcal{A})$  is uniformly bounded and clustered around 1 and the results indicate that the estimates in Theorems 3.4 and 3.5 are sharp.

**3.3. Time-varying and nonlinear case: NKPA technique.** For the linear case with time-varying coefficient matrix  $K(t)$ , the all-at-once matrix for the Sinc-Nyström method is

$$\mathcal{A} = I_m \otimes I_n - ((I^{(-1)}D) \otimes I_n)\mathbb{K}, \quad (3.14)$$

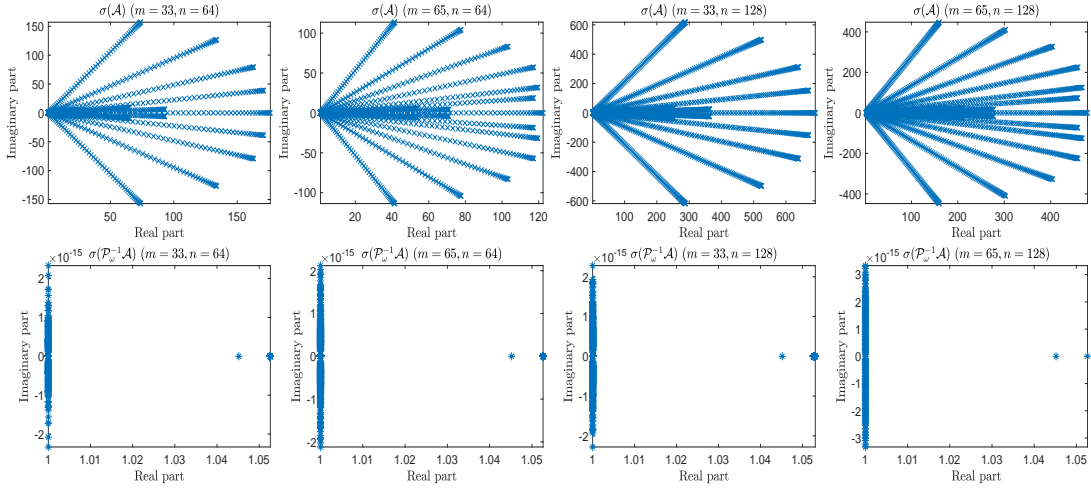


FIG. 3.5. The eigenvalues of  $\mathcal{A}$  and  $\mathcal{P}^{-1}(\omega)\mathcal{A}$  with  $\omega = 0.1$  for 1D heat equation with  $n = 64, 128$  and  $m = 33, 65$ . Notice that all the eigenvalues of  $\mathcal{P}^{-1}(\omega)\mathcal{A}$  are real and located in the interval  $[1, \frac{1}{1-\omega}) = [1, \frac{1}{0.9})$ .

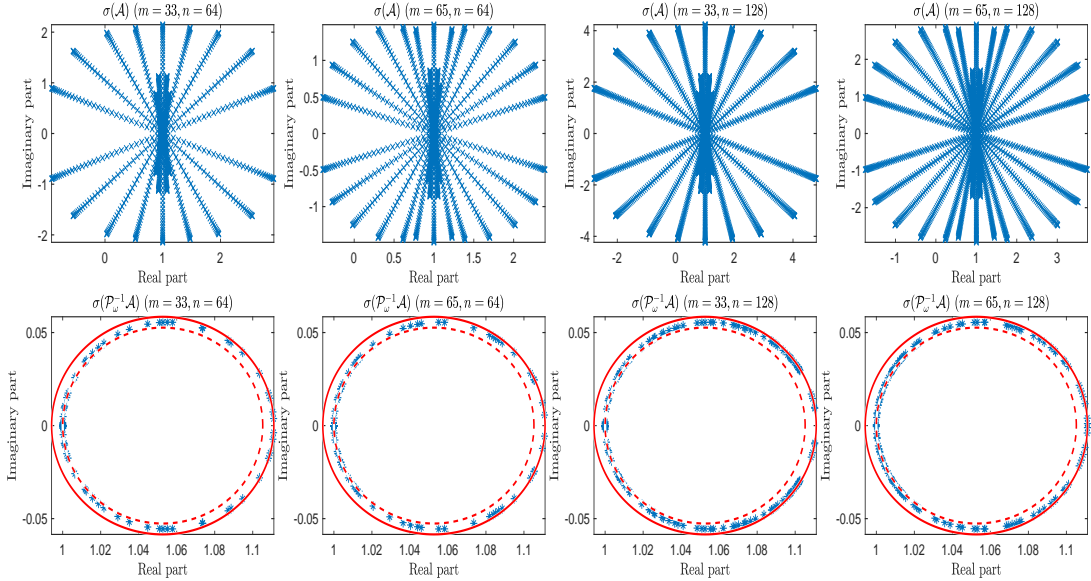


FIG. 3.6. The eigenvalues of  $\mathcal{A}$  and  $\mathcal{P}^{-1}(\omega)\mathcal{A}$  with  $\omega = 0.1$  for 1D wave equation with  $n = 64, 128$  and  $m = 33, 65$ . Notice that all the eigenvalues of  $\mathcal{P}^{-1}(\omega)\mathcal{A}$  are locate within an annulus  $\mathbb{A}_\omega$  (with center  $(\frac{2}{2-\omega}, 0)$ , inner circle radius  $\frac{\omega}{(2-\omega)}$  in dashed line, outer circle radius  $\frac{\omega}{(2-\omega)(1-\omega)}$  in solid line).

where  $\mathbb{K} = \text{blkdiag}(K(t_{-M}), \dots, K(t_M))$ . To get a diagonalization-based PinT preconditioner, the widely used approach is to follow the idea in [12] to construct an approximation (of tensor structure) to  $\mathbb{K}$ , such as

$$\mathbb{K} \approx I_m \otimes \bar{K}, \quad \bar{K} := \frac{1}{m} \sum_{j=-M}^M K(t_j), \quad (3.15)$$

where  $m = 2M + 1$ . This leads to preconditioner

$$\overline{\mathcal{P}} = I_m \otimes I_n - (SD \otimes I_n)(I_m \otimes \overline{K}) = I_m \otimes I_n - (SD \otimes \overline{K}), \quad (3.16)$$

which is of the same structure as  $\mathcal{P}$  in (3.2) and therefore the diagonalization-based PinT procedure (3.4) is applicable to  $\overline{\mathcal{P}}$  as well. Such an *averaging*-based Kronecker product approximation works well when  $K(t)$  does not change dramatically over the considered time interval. However, if  $K(t)$  has very large variance on the Sinc time points, using the preconditioner  $\overline{\mathcal{P}}$  may result in slow convergence rate or even divergence for the GMRES method. Here we propose another approximation of  $\mathbb{K}$  based on the nearest Kronecker product approximation (NKPA) technique. The idea lies in approximating  $\mathbb{K}$  by a tensor structure matrix  $\hat{D} \otimes \overline{K}$  with diagonal matrix  $\hat{D}$  fixed by

$$\min_{\hat{D} \text{ is diagonal}} \|\mathbb{K} - \hat{D} \otimes \overline{K}\|, \quad (3.17)$$

where  $\overline{K}$  is the averaging matrix given in (3.15). Under the Frobenius norm  $\|\cdot\|_F$ , according to [45, Thm. 3] the solution  $\hat{D} = \text{diag}(D_1, \dots, D_m)$  of (3.17) has an explicit formula

$$\hat{D}_j = \frac{\text{trace}(K(t_j)^T \overline{K})}{\text{trace}(\overline{K}^T \overline{K})}, \quad j = 1, 2, \dots, m, \quad (3.18)$$

where  $\text{trace}(\overline{K}^T \overline{K}) > 0$  is assumed. This gives the following preconditioner

$$\hat{\mathcal{P}} = I_m \otimes I_n - (SD \otimes I_n)(\hat{D} \otimes \overline{K}) = I_m \otimes I_n - (SD\hat{D} \otimes \overline{K}), \quad (3.19)$$

which is also of the same structure as  $\mathcal{P}$  in (3.2) since  $D\hat{D}$  is a diagonal matrix. Numerically, we find that such an improved preconditioner often results in a significantly faster convergence rate than the averaging-based preconditioner  $\overline{\mathcal{P}}$ , especially when  $\hat{D}$  deviates largely from the identity matrix  $I_m$  (i.e.,  $K(t)$  undergoes a large variance over the Sinc collation time points). For the case that  $K(t) = K$  is constant,  $\overline{\mathcal{P}}$  and  $\hat{\mathcal{P}}$  are identical. Clearly, the diagonalization procedure (3.4) also applies to  $\hat{\mathcal{P}}$ . However, the spectrum analysis of the preconditioned matrices  $\overline{\mathcal{P}}^{-1}\mathcal{A}$  and  $\hat{\mathcal{P}}^{-1}\mathcal{A}$  becomes extremely difficult and further discussion on this is beyond the scope of this paper. Analogous to the definition of  $\mathcal{P}(\omega)$ , we can also define  $\hat{\mathcal{P}}(\omega)$  as

$$\hat{\mathcal{P}}(\omega) = I_m \otimes I_n - (S(\omega)D \otimes I_n)(\hat{D} \otimes \overline{K}) = I_m \otimes I_n - (S(\omega)D\hat{D} \otimes \overline{K}), \quad (3.20)$$

which is expected to perform better than  $\hat{\mathcal{P}}$  when  $\omega \in (0, 1)$  is small.

In the nonlinear case, the block-diagonal matrix  $\mathbf{Q}(\mathbf{y}_h)$  in (2.14) shares the same block-diagonal structure as  $\mathbb{K}$  and thus the aforementioned NKPA technique can be used, too. This observation naturally leads to a similar NKPA-based preconditioner for the GMRES method used as an inner solver within the Newton iteration (2.15) for solving the Jacobian system.

**4. Numerical examples.** In this section, we present numerical results to illustrate the effectiveness of our proposed preconditioners. All simulations are implemented using MATLAB on a Dell Precision 5820 Tower Workstation with Intel(R) Core(TM) i9-10900X 3.70GHz CPU and 64GB RAM. The CPU time (in seconds) is estimated by using the timing functions `tic/toc`, based on the serial implementation of the preconditioned iterative algorithms. We employ the right-preconditioned GMRES [40] solver (without restarts) in the IFISS package [7, 8, 42], and choose a zero initial guess and a small stopping tolerance  $\text{tol} = 10^{-10}$  (for high order accuracy purpose) based on the reduction in relative residual norms. The number of GMRES iterations for achieving the stopping tolerance is denoted by  $\text{It}_G$ . We will take  $d = \pi/2$  and



$\alpha = 1$  in the Sinc-Nyström method. In measuring the accuracy of the Sinc-Nyström method, we will report the maximum error (denoted by ‘Error’) between Sinc approximation and the exact solution (if known) over all non-uniform Sinc time points.

For both the heat and wave equations, We discretize the Laplacian operator  $\Delta$  by a centered difference scheme in space with a uniform mesh step size  $h_x$  to get the discrete Laplacian matrix  $\Delta_{h_x}$ . For all numerical experiments, the preconditioners proposed in this paper are used according to the diagonalization procedure (3.4). In rectangular domains with regular grids, the complex-shifted systems in Step-(ii) of (3.4) are solved in serial by MATLAB’s sparse direct solver (Thomas algorithm) and fast Poisson direct solver [39] (based on discrete sine transform) for 1D and 2D cases, respectively. For more general domains with irregular grids (e.g., finite element discretization), fast iterative solvers (e.g., the multigrid method [2, 22, 47], the domain decomposition method [18] and the preconditioned GMRES method [11]) can be used.

**Example 1: linear 2D heat equation with constant coefficients.** We first consider the following 2D heat equation defined on the space domain  $\Omega = (0, \pi)^2$ :

$$\begin{cases} y_t = \Delta y + g, & \text{in } \Omega \times (0, T), \\ y = 0, & \text{on } \partial\Omega \times (0, T), \end{cases} \quad (4.1)$$

where the initial condition  $y(x_1, x_2, 0) = x_1(\pi - x_1)x_2(\pi - x_2)$  and source term  $g$  are chosen such that the exact solution is  $y(x_1, x_2, t) = x_1(\pi - x_1)x_2(\pi - x_2)e^{-t}$ . Table 4.1 shows the error and convergence results for the GMRES method without preconditioner (denoted as ‘None’) and with our PinT preconditioners  $\mathcal{P}$  and  $\mathcal{P}(\omega)$  (with  $\omega = 0.01$ ), respectively. With the preconditioner  $\mathcal{P}$  only a few iterations is sufficient to achieve stopping tolerance. Such a fast convergence rate is anticipated from the highly clustered spectrum distribution of  $\mathcal{P}^{-1}\mathcal{A}$  given in Theorem 3.3. Interestingly, for a fixed  $n$  (e.g.  $n = 32^2$ ) we do observe that  $\text{It}_G$  slightly decreasing as  $m$  increases, which is reasonable since  $\mathcal{P}^{-1}\mathcal{A}$  has only  $n$  non-unity eigenvalues regardless of  $m$ . For this example, the improved preconditioner  $\mathcal{P}(\omega = 0.01)$  shows almost the same convergence rate as  $\mathcal{P}$ , which is anticipated since the spectrum of  $\mathcal{P}^{-1}\mathcal{A}$  is already highly clustered, as shown in Figures 3.3 and 3.5. Nevertheless, for  $m = 257$  the Error corresponding to  $\mathcal{P}(\omega = 0.01)$  seems to slightly larger than that by  $\mathcal{P}$ , which is due to a larger roundoff error during diagonalization.

TABLE 4.1  
Results for Example 1 (2D heat PDE with constant coefficients,  $T = 2, \text{tol} = 10^{-10}$ )

$n$	$m$	None			$\mathcal{P}$			$\mathcal{P}(\omega)$ with $\omega = 0.01$		
		Error	$\text{It}_G$	CPU	Error	$\text{It}_G$	CPU	Error	$\text{It}_G$	CPU
$32^2$	33	1.3e-03	682	15.30	1.3e-03	4	0.04	1.3e-03	3	0.03
	65	3.5e-05	663	23.52	3.5e-05	3	0.06	3.5e-05	3	0.06
	129	2.0e-07	596	177.73	2.1e-07	3	0.15	2.0e-07	3	0.16
	257	5.0e-09	531	230.47	2.9e-10	3	0.34	4.2e-08	3	0.33
$64^2$	33	>1000			1.3e-03	4	0.14	1.3e-03	3	0.11
	65	>1000			3.5e-05	3	0.21	3.5e-05	3	0.21
	129	>1000			2.1e-07	3	0.45	2.1e-07	3	0.43
	257	>1000			2.9e-10	3	1.03	4.4e-08	3	1.02
$128^2$	33	>1000			1.3e-03	5	0.61	1.3e-03	3	0.38
	65	>1000			3.5e-05	3	0.81	3.5e-05	3	0.78
	129	>1000			2.1e-07	3	1.73	2.1e-07	3	1.74
	257	>1000			2.9e-10	3	4.02	5.2e-08	3	4.06

**Example 2: linear 2D heat equation with time-varying coefficients.** We next consider a linear 2D heat equation with time-varying coefficient on  $\Omega = (0, \pi)^2$ :

$$\begin{cases} y_t = \kappa(t)\Delta y, & \text{in } \Omega \times (0, T), \\ y = 0, & \text{on } \partial\Omega \times (0, T), \end{cases} \quad (4.2)$$

where  $\kappa(t) = 1/((1.2+t)\ln(1.2+t))$  and the initial condition  $y(\cdot, 0)$  is chosen such that the exact solution is  $y(x_1, x_2, t) = x_1(\pi - x_1)x_2(\pi - x_2)/\ln(1.2+t)$ . In Figure 4.1 we plot the eigenvalues of  $\mathcal{A}$ ,  $\overline{\mathcal{P}}^{-1}\mathcal{A}$  and  $\widehat{\mathcal{P}}^{-1}\mathcal{A}$  for a fixed space-time mesh ( $m = 33$  and  $n = 16^2 = 256$ ). For  $\overline{\mathcal{P}}$  we compute the diagonal matrix  $\widehat{D}$  according to the formula (3.18) and from Figure 4.1 on the top right we see that such a diagonal matrix is indeed very different from an identity matrix. From the two subfigures on the bottom row we see that the eigenvalues of  $\widehat{\mathcal{P}}^{-1}\mathcal{A}$  are more clustered than that of  $\overline{\mathcal{P}}^{-1}\mathcal{A}$ .

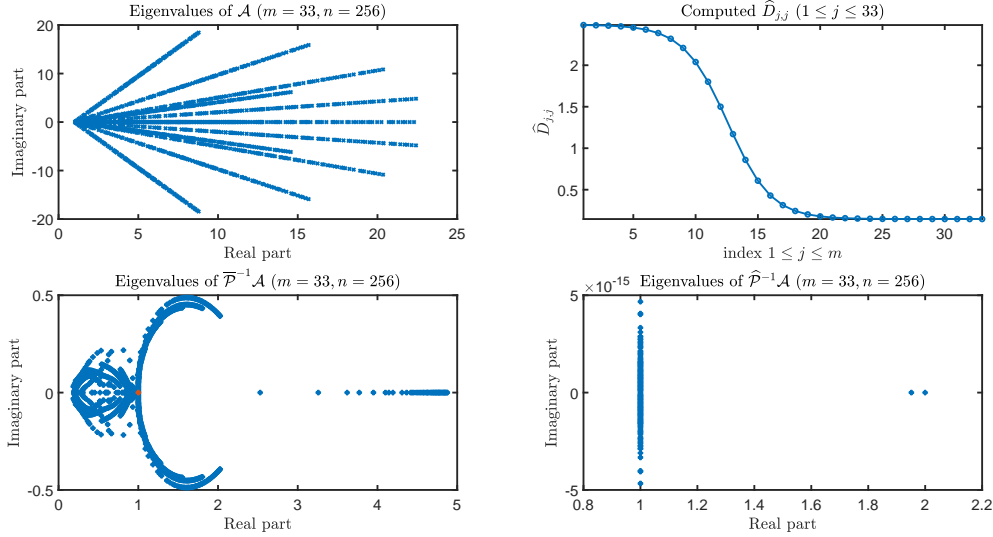


FIG. 4.1. The eigenvalue distribution of  $\mathcal{A}$ ,  $\overline{\mathcal{P}}^{-1}\mathcal{A}$ , and  $\widehat{\mathcal{P}}^{-1}\mathcal{A}$  and  $\widehat{D}$  for Example 2 (2D time-varying case).

In Table 4.2 we report the errors and convergence results for the GMRES method without preconditioner and with two PinT preconditioners  $\overline{\mathcal{P}}$  and  $\widehat{\mathcal{P}}$ . It is clear that the NKPA-based preconditioner  $\widehat{\mathcal{P}}$  in (3.19) leads to faster convergence rate than the averaging-based preconditioner  $\overline{\mathcal{P}}$  given by (3.16). This result confirms very well the eigenvalue distribution of  $\overline{\mathcal{P}}^{-1}\mathcal{A}$  and  $\widehat{\mathcal{P}}^{-1}\mathcal{A}$  in Figure 4.1. We also tested the GMRES method using the preconditioner  $\widehat{\mathcal{P}}(\omega)$  with  $\omega = 0.01$ , but the results are very similar to that of  $\widehat{\mathcal{P}}$ . So we omit the presentation.

**Example 3: linear 2D wave equation.** We now consider a linear 2D wave equation defined on  $\Omega = (0, \pi)^2$ :

$$\begin{cases} y_{tt} = \Delta y + g, & \text{in } \Omega \times (0, T), \\ y = 0, & \text{on } \partial\Omega \times (0, T), \end{cases} \quad (4.3)$$

where the initial conditions  $y(\cdot, 0)$  and  $y_t(\cdot, 0)$  are fixed according to the exact solution  $y(x_1, x_2, t) = x_1(\pi - x_1)x_2(\pi - x_2)\ln(1+t)$ . By defining  $p = y_t$ , this second-order wave equation can be reduced

TABLE 4.2  
Results for Example 2 (2D heat PDE with time-varying coefficients,  $T = 2$ ,  $\text{tol} = 10^{-10}$ )

$n$	$m$	None			$\overline{\mathcal{P}}$			$\widehat{\mathcal{P}}$		
		Error	It <sub>G</sub>	CPU	Error	It <sub>G</sub>	CPU	Error	It <sub>G</sub>	CPU
$32^2$	33	3.2e-02	669	15.48	3.2e-02	69	0.76	3.2e-02	4	0.05
	65	8.9e-04	628	21.92	8.9e-04	68	1.52	8.9e-04	3	0.08
	129	5.1e-06	552	148.42	5.1e-06	69	5.06	5.1e-06	3	0.17
	257	2.7e-08	488	223.90	1.5e-08	69	10.66	6.7e-09	3	0.41
$64^2$	33	>1000			3.2e-02	73	4.59	3.2e-02	4	0.18
	65	>1000			8.9e-04	71	8.32	8.9e-04	3	0.29
	129	>1000			5.1e-06	71	15.05	5.1e-06	3	0.60
	257	>1000			1.7e-08	71	34.35	6.7e-09	3	1.38
$128^2$	33	>1000			3.2e-02	81	18.45	3.2e-02	5	0.78
	65	>1000			8.9e-04	72	30.52	8.9e-04	4	1.35
	129	>1000			5.1e-06	72	64.18	5.2e-06	3	2.46
	257	>1000			1.7e-08	72	140.85	6.6e-09	3	5.50

to a first-order PDE system:

$$\begin{cases} y_t = p; & \text{in } \Omega \times (0, T), \\ p_t = \Delta y + g, & \text{in } \Omega \times (0, T), \\ y = 0, p = 0 & \text{on } \partial\Omega \times (0, T). \end{cases} \quad (4.4)$$

By applying the centered finite difference in space with a uniform mesh step size  $h_x$  to (4.4), we obtain a linear ODE system with a  $2n \times 2n$  sparse constant coefficient matrix

$$K = \begin{bmatrix} \mathbf{0} & I_n \\ \Delta_{h_x} & \mathbf{0} \end{bmatrix} \in \mathbb{R}^{2n \times 2n}.$$

In Table 4.3, we present the errors and convergence results of the GMRES method without preconditioner and with the proposed preconditioner  $\mathcal{P}$  and  $\mathcal{P}(\omega)$  (with  $\omega = 0.01$ ). In contrast to the above heat equations, the GMRES method without preconditioner does not converge within 1000 iterations for all combinations of  $n$  and  $m$ . Fortunately, the improved preconditioner  $\mathcal{P}(\omega)$  with a moderate parameter  $\omega = 0.01$  can achieve much faster mesh-independent convergence rates, which confirms Theorem 3.5 very well.

TABLE 4.3  
Results for Example 3 (2D wave PDE,  $T = 2$ ,  $\text{tol} = 10^{-10}$ )

$2n$	$m$	None			$\mathcal{P}(\omega)$ with $\omega = 0.01$		
		Error	It <sub>G</sub>	CPU	Error	It <sub>G</sub>	CPU
$2 \times 32^2$	33	>1000			1.8e-03	5	0.07
	65	>1000			4.9e-05	5	0.16
	129	>1000			2.8e-07	5	0.39
	257	>1000			4.1e-10	5	0.78
$2 \times 64^2$	33	>1000			1.8e-03	5	0.25
	65	>1000			4.9e-05	5	0.55
	129	>1000			2.8e-07	5	1.20
	257	>1000			4.3e-10	5	2.76

The preconditioner  $\mathcal{P}(\omega)$  contains a free parameter  $\omega$  and in Figure 3.4 we have plotted the condition number of the eigenvector matrix of  $S(\omega)D$  for different values of  $\omega$ . As we mentioned

there, such a condition number is proportional to the roundoff error arising from the diagonalization procedure (3.4) and a large roundoff error will seriously pollute the discretization accuracy. So, it would be interesting to illustrate how the parameter  $\omega$  affects discretization accuracy in practice. In Table 4.4 we report the errors and convergence results of the GMRES method with NKPA-based preconditioner  $\mathcal{P}(\omega)$  for a set of values of  $\omega$ . We see that for the first few  $\omega$  the iteration number decreases as  $\omega$  decreases, but it re-bounces when  $\omega \leq 10^{-9}$ . From the results for Error, we see that the roundoff error due to the diagonalization procedure quickly contaminate the discretization accuracy. In particular, for  $\omega = 10^{-15}$  the measured Error is very bad. This can be explained as follows. For such a small  $\omega$ ,  $\mathcal{P}(\omega)$  approximately equals to  $I^{-1}D$ , so applying the diagonalization procedure to  $\mathcal{P}(\omega)$  is equivalent to diagonalizing  $I^{-1}D$  (as  $I^{-1}D = U\Psi U^{-1}$ ), which is unstable due to a very large condition number of  $U$  (cf. Figure 3.4). For this example, it seems  $\omega \approx 10^{-6}$  is the best choice.

TABLE 4.4  
Results for Example 3 with the improved preconditioner  $\mathcal{P}(\omega)$  (2D wave PDE,  $T = 2, \text{tol} = 10^{-10}$ )

$2n$	$m$	$\omega = 10^{-3}$		$\omega = 10^{-6}$		$\omega = 10^{-9}$		$\omega = 10^{-12}$		$\omega = 10^{-15}$	
		Error	It <sub>G</sub>	Error	It <sub>G</sub>	Error	It <sub>G</sub>	Error	It <sub>G</sub>	Error	It <sub>G</sub>
$2 \times 32^2$	33	1.8e-03	3	1.8e-03	2	1.8e-03	2	1.8e-03	2	1.8e-03	2
	65	4.9e-05	3	4.9e-05	2	4.9e-05	2	1.3e-04	3	7.1e-05	3
	129	2.8e-07	3	2.8e-07	2	9.7e-07	2	3.6e-04	3	2.3e-01	10
	257	9.9e-10	3	1.6e-09	2	1.1e-06	3	7.4e-04	35	7.1e-01	10
$2 \times 64^2$	33	1.8e-03	3	1.8e-03	2	1.8e-03	2	1.8e-03	2	1.8e-03	2
	65	4.9e-05	3	4.9e-05	2	4.9e-05	2	1.2e-04	3	7.4e-05	3
	129	2.9e-07	3	2.8e-07	2	9.4e-07	2	4.0e-04	3	1.8e-01	10
	257	1.0e-09	3	1.7e-09	2	1.0e-06	3	6.0e-04	40	5.7e-01	10
$2 \times 128^2$	33	1.8e-03	3	1.8e-03	2	1.8e-03	2	1.8e-03	2	1.8e-03	2
	65	4.9e-05	3	4.9e-05	2	4.9e-05	2	1.7e-04	3	7.6e-05	3
	129	2.9e-07	3	2.8e-07	2	1.1e-06	2	3.8e-04	3	1.6e-01	10
	257	1.1e-09	3	1.1e-09	2	8.4e-07	3	5.1e-04	39	5.6e-01	9

**Example 4: Allen–Cahn equation.** At the end of this section, we consider the 1D Allen–Cahn equation [23] on a spatial domain  $\Omega = (-1, 1)$ :

$$\begin{cases} y_t = 0.01y_{xx} + y - y^3, & \text{in } \Omega \times (0, T), \\ y(-1, t) = -1, \quad y(1, t) = 1, & \text{in } (0, T), \\ y(x, 0) = 0.53x + 0.47 \sin(-1.5\pi x), & \text{in } \Omega. \end{cases} \quad (4.5)$$

We first apply the centered finite difference scheme with a uniform mesh step size  $h_x$  to get a nonlinear ODE system, for which the nonlinear Sinc-Nyström system is solved by Newton’s method (2.15) with zero initial guess, where the Jacobian system for each Newton iteration is solved by GMRES without preconditioner and with the NKPA-based preconditioner  $\widehat{\mathcal{P}}$ , respectively. In Table 4.5, we show the errors and iteration numbers for Newton’s method (denoted by It<sub>N</sub>) and the maximal iteration number of the GMRES method over all the Newton iterations (denoted by It<sub>G</sub>). While costing the same number of outer Newton iterations, the preconditioner  $\widehat{\mathcal{P}}$  leads to much faster convergence for the GMRES method and much less CPU time. Notice that It<sub>G</sub> for GMRES without preconditioner increases dramatically as the spatial size  $n$  grows. (The results for the preconditioner  $\overline{\mathcal{P}}$  defined by (3.16) is omitted since it gives the same It<sub>G</sub> as  $\widehat{\mathcal{P}}$ , perhaps due to small variance of the solution in time.) With a generalized version of  $\widehat{\mathcal{P}}$ , i.e.,  $\widehat{\mathcal{P}}(\omega)$  with  $\omega = 0.01$ , we see in Table 4.5 that both It<sub>G</sub> and the CPU time can be further reduced.

TABLE 4.5  
Results for Example 1 (1D Allen-Cahn PDE,  $T = 2$ ,  $\text{tol} = 10^{-10}$ )

$n$	$m$	None				$\hat{\mathcal{P}}$				$\hat{\mathcal{P}}(\omega)$ with $\omega = 0.01$			
		Error	It <sub>N</sub>	It <sub>G</sub>	CPU	Error	It <sub>N</sub>	It <sub>G</sub>	CPU	Error	It <sub>N</sub>	It <sub>G</sub>	CPU
256	33	2.6e-05	5	473	16.64	2.6e-05	5	14	0.22	2.6e-05	5	7	0.13
	65	4.7e-07	5	419	20.28	4.7e-07	5	14	0.42	4.7e-07	5	7	0.26
	129	1.9e-09	5	362	24.90	1.9e-09	5	14	1.01	1.9e-09	5	7	0.55
	257	1.5e-11	5	314	35.86	1.4e-11	5	14	2.36	1.4e-11	5	7	1.30
512	33			>1000		2.6e-05	5	14	0.68	2.6e-05	5	7	0.50
	65			>1000		4.7e-07	5	14	1.29	4.7e-07	5	7	0.97
	129			>1000		1.9e-09	5	14	2.95	1.9e-09	5	7	2.06
	257			>1000		1.4e-11	5	14	7.05	1.4e-11	5	7	4.68
1024	33			>1000		2.6e-05	5	14	1.99	2.6e-05	5	7	1.28
	65			>1000		4.7e-07	5	14	3.95	4.7e-07	5	7	3.38
	129			>1000		1.9e-09	5	14	9.28	1.9e-09	5	7	7.12
	257			>1000		1.4e-11	5	14	19.50	1.4e-11	5	7	14.72

Since the exact solution is unknown, we compute the reference solution by using MATLAB's ODE solver `ode15s` with a very small tolerance  $10^{-12}$  and the same space-time mesh. As expected, the reported errors in Table 4.5 shows an exponential order of accuracy in time. Figure 4.2 illustrates the reference and approximate solutions, where we see clearly how the non-uniform Sinc mesh points in time cluster near  $t = 0$  and  $t = T$ .

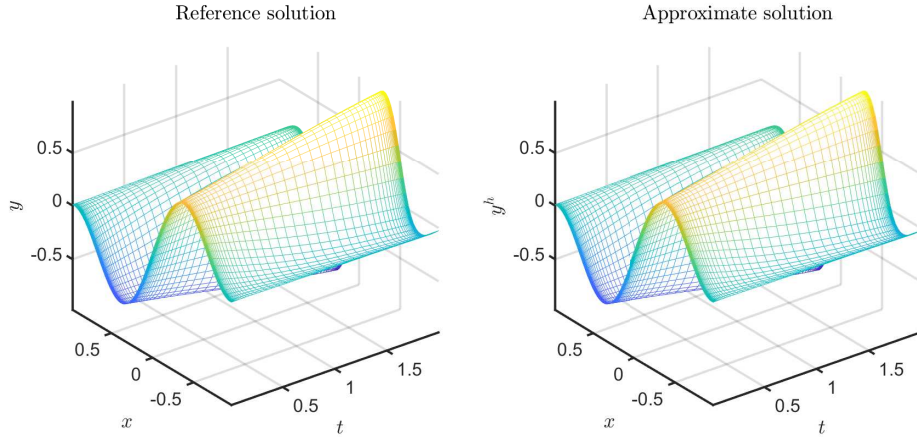


FIG. 4.2. The reference and Sinc approximation for Example 4 (1D Allen-Cahn PDE) with  $m = 257$ ,  $n = 64$ .

**5. Conclusion.** The Sinc-Nyström method for the initial-value ODEs can achieve exponential order of accuracy in time and for this method the linear (or nonlinear) all-at-once system is the major problem that we need to handle in practice. In this paper, we proposed some efficient preconditioners for solving such an all-at-once system for both the parabolic and hyperbolic problems. The construction of the preconditioner is based on looking insight into a special structure of the discretization matrix of the Sinc-Nyström method, namely the *Toeplitz-times-diagonal* structure. The spectrum analysis and the extensive numerical results indicate that the preconditioned GMRES method has mesh-independent convergence rates. Moreover,

if parallel computer is available, the proposed preconditioners can be used in parallel for all the Sinc time points, following a block diagonalization procedure (cf. (3.4)). We have shown that this idea works, because such a diagonalization is well conditioned, i.e., the condition number of the eigenvector matrix of the block diagonalization is a moderate quantity and only weakly grows as the number of Sinc time points increases (cf. Figure 3.4).

It would be interesting to generalize this work to other spectral methods (e.g. Chebyshev method). In the previous work [28, 44], it was shown that these methods can be very useful in improving the accuracy in time of the numerical solutions, but the large scale all-at-once system could be a serious problem for applying these methods to time-dependent PDEs. Such a generalization is by no means trivial, because the structure of all-at-once matrix is completely different from that of the Sinc-Nyström method and therefore the construction of the preconditioner and the spectral analysis of the preconditioned matrix need new ideas.

**Acknowledgement.** The authors would like to thank Dr. Xiang-Sheng Wang from University of Louisiana at Lafayette for pointing out a flaw in the proof of Lemma 3.2.

#### REFERENCES

- [1] I. T. ABU-JEIB AND T. S. SHORES, *On properties of matrix  $I^{(-1)}$  of Sinc methods*, New Zealand J. Math, 32 (2003), pp. 1–10.
- [2] L. BANJAI AND D. PETERSEIM, *Parallel multistep methods for linear evolution problems*, IMA Journal of Numerical Analysis, 32 (2011), pp. 1217–1240(24).
- [3] B. BIALECKI, *Sinc-Nyström method for numerical solution of a dominant system of cauchy singular integral equations given on a piecewise smooth contour*, SIAM Journal on Numerical Analysis, 26 (1989), pp. 1194–1211.
- [4] B. BIALECKI AND F. STENGER, *Sinc-Nyström method for numerical solution of one-dimensional cauchy singular integral equation given on a smooth arc in the complex plane*, Mathematics of Computation, 51 (1988), pp. 133–165.
- [5] A. CHRISTLIEB AND B. ONG, *Implicit parallel time integrators*, Journal of Scientific Computing, 49 (2011), pp. 167–179.
- [6] F. DANIELI, B. S. SOUTHWORTH, AND A. J. WATHEN, *Space-time block preconditioning for incompressible flow*, arXiv (2021): 2005.09158 (<http://arxiv.org/abs/2101.07003v1>).
- [7] H. ELMAN, A. RAMAGE, AND D. SILVESTER, *Algorithm 866: IFISS, a Matlab toolbox for modelling incompressible flow*, ACM Transactions on Mathematical Software, 33 (2007), pp. 2–14.
- [8] ———, *IFISS: A computational laboratory for investigating incompressible flow problems*, SIAM Review, 56 (2014), pp. 261–273.
- [9] R. D. FALGOUT, S. FRIEDHOFF, T. V. KOLEV, S. P. MACLACHLAN, AND J. B. SCHRODER, *Parallel time integration with multigrid*, SIAM Journal on Scientific Computing, 36 (2014), pp. C635–C661.
- [10] M. J. GANDER, *50 years of time parallel time integration*, in Multiple shooting and time domain decomposition methods, Springer, 2015, pp. 69–113.
- [11] M. J. GANDER, I. G. GRAHAM, AND E. A. SPENCE, *Applying GMRES to the Helmholtz equation with shifted laplacian preconditioning: what is the largest shift for which wavenumber-independent convergence is guaranteed?*, Numerische Mathematik, 131 (2015), pp. 567–614.
- [12] M. J. GANDER AND L. HALPERN, *Time parallelization for nonlinear problems based on diagonalization*, in Domain Decomposition Methods in Science and Engineering XXIII, Springer, 2017, pp. 163–170.
- [13] M. J. GANDER, L. HALPERN, J. RANNOU, AND J. RYAN, *A direct time parallel solver by diagonalization for the wave equation*, SIAM Journal on Scientific Computing, 41 (2019), pp. A220–A245.
- [14] M. J. GANDER, J. LIU, S.-L. WU, X. YUE, AND T. ZHOU, *ParaDiag: Parallel-in-time algorithms based on the diagonalization technique*, arXiv (2021): 2005.09158 (<http://arxiv.org/abs/2005.09158>).
- [15] M. J. GANDER AND S.-L. WU, *Convergence analysis of a periodic-like waveform relaxation method for initial-value problems via the diagonalization technique*, Numerische Mathematik, 143 (2019), pp. 489–527.
- [16] A. GODDARD AND A. WATHEN, *A note on parallel preconditioning for all-at-once evolutionary PDEs*, Electronic Transactions on Numerical Analysis, 51 (2019), pp. 135–150.
- [17] G. GOLUB AND C. VAN LOAN, *Matrix Computations*, Matrix Computations, Johns Hopkins University Press, 2012.
- [18] I. G. GRAHAM, E. A. SPENCE, AND E. VAINIKKO, *Domain decomposition preconditioning for high-frequency Helmholtz problems with absorption*, Mathematics of Computation, 86 (2015), pp. 2559–2604.

- [19] A. GREENBAUM, V. PTÁK, AND Z. E. K. STRAKOŠ, *Any nonincreasing convergence curve is possible for GMRES*, SIAM Journal on Matrix Analysis and Applications, 17 (1996), pp. 465–469.
- [20] L. HAN AND J. XU, *Proof of Stenger’s conjecture on matrix  $I^{(-1)}$  of Sinc methods*, Journal of Computational and Applied Mathematics, 255 (2014), pp. 805–811.
- [21] R. HARA AND T. OKAYAMA, *Error analyses of Sinc-Nyström methods for initial value problems*, Nonlinear Theory and Its Applications, IEICE, 10 (2019), pp. 465–484.
- [22] L. R. HOCKING AND C. GREIF, *Optimal complex relaxation parameters in multigrid for complex-shifted linear systems*, SIAM Journal on Matrix Analysis and Applications, 42 (2021), pp. 475–502.
- [23] A.-K. KASSAM AND L. N. TREFETHEN, *Fourth-order time-stepping for stiff PDEs*, SIAM Journal on Scientific Computing, 26 (2005), pp. 1214–1233.
- [24] F.-R. LIN, X. LU, AND X.-Q. JIN, *Sinc-Nyström method for singularly perturbed Love’s integral equation*, East Asian Journal on Applied Mathematics, 3 (2013), pp. 48–58.
- [25] X. L. LIN, M. K. NG, AND Y. ZHI, *A parallel-in-time two-sided preconditioning for all-at-once system from a non-local evolutionary equation with weakly singular kernel*, Journal of Computational Physics, 434 (2021), p. 110221.
- [26] J.-L. LIONS, Y. MADAY, AND G. TURINICI, *A “parareal” in time discretization of PDE’s*, Comptes Rendus de l’Académie des Sciences - Series I - Mathematics, 332 (2001), pp. 661–668.
- [27] J. LIU AND S. L. WU, *A fast block  $\alpha$ -circulant preconditioner for all-at-once systems from wave equations*, SIAM Journal on Matrix Analysis and Applications, 41 (2020), pp. 1912–1943.
- [28] S. H. LUI AND S. NATAJ, *Spectral collocation in space and time for linear pdes*, Journal of Computational Physics, 424 (2021), p. 109843.
- [29] Y. MADAY AND E. M. RÖNQUIST, *Parallelization in time through tensor-product space-time solvers*, Comptes Rendus Mathématique, 346 (2008), pp. 113–118.
- [30] E. McDONALD, J. PESTANA, AND A. WATHEN, *Preconditioning and iterative solution of all-at-once systems for evolutionary partial differential equations*, SIAM Journal on Scientific Computing, 40 (2018), pp. A1012–A1033.
- [31] C. MEHL, V. MEHRMANN, A. RAN, AND L. RODMAN, *Eigenvalue perturbation theory of classes of structured matrices under generic structured rank one perturbations*, Linear Algebra and its Applications, 435 (2011), pp. 687–716.
- [32] G. MEURANT AND J. D. TEBBENS, *The role eigenvalues play in forming GMRES residual norms with non-normal matrices*, Numerical Algorithms, 68 (2015), pp. 143–165.
- [33] M. K. NG, *Circulant and skew-circulant splitting methods for Toeplitz systems*, Journal of Computational and Applied Mathematics, 159 (2003), pp. 101–108.
- [34] T. OKAYAMA, *Theoretical analysis of Sinc-collocation methods and Sinc-Nyström methods for systems of initial value problems*, BIT Numerical Mathematics, 58 (2018), pp. 199–220.
- [35] T. OKAYAMA, T. MATSUO, AND M. SUGIHARA, *Error estimates with explicit constants for Sinc approximation, Sinc quadrature and Sinc indefinite integration*, Numerische Mathematik, 124 (2013), pp. 361–394.
- [36] ———, *Theoretical analysis of Sinc-Nyström methods for volterra integral equations*, Mathematics of Computation, 84 (2015), pp. 1189–1215.
- [37] B. W. ONG AND R. J. SPITERI, *Deferred correction methods for ordinary differential equations*, Journal of Scientific Computing, 83 (2020), pp. 1–29.
- [38] A. RAHMOUNE AND A. GUECHI, *Sinc-Nyström methods for Fredholm integral equations of the second kind over infinite intervals*, Applied Numerical Mathematics, 157 (2020), pp. 579–589.
- [39] Y. SAAD, *Iterative Methods for Sparse Linear Systems: Second Edition*, SIAM, Philadelphia, PA, 2003.
- [40] Y. SAAD AND M. H. SCHULTZ, *GMRES: A generalized minimal residual algorithm for solving nonsymmetric linear systems*, SIAM Journal on Scientific and Statistical Computing, 7 (1986), pp. 856–869.
- [41] SHU-LIN, *Toward parallel coarse grid correction for the parareal algorithm*, SIAM Journal on Scientific Computing, 40 (2018), pp. A1446–A1472.
- [42] D. SILVESTER, H. ELMAN, AND A. RAMAGE, *Incompressible Flow and Iterative Solver Software (IFISS) version 3.6*, November 2021. <http://www.manchester.ac.uk/ifiss/>.
- [43] F. STENGER, *Numerical methods based on Sinc and analytic functions*, vol. 20, Springer Series in Computational Mathematics, Springer-Verlag, 2012.
- [44] T. TAO AND X. XIANG, *Accuracy enhancement using spectral postprocessing for differential equations and integral equations*, Communications in Computational Physics, 5 (2008), pp. 779–792.
- [45] C. F. VAN LOAN AND N. PITSIANIS, *Approximation with Kronecker products*, in Linear algebra for large scale and real-time applications, Springer, 1993, pp. 293–314.
- [46] A. J. WATHEN, *Preconditioning*, Acta Numerica, 24 (2015), pp. 329–376.
- [47] S. L. WU, H. ZHANG, AND T. ZHOU, *Solving time-periodic fractional diffusion equations via diagonalization technique and multigrid*, Numerical Linear Algebra with Applications, (2018), p. e2178.